Cell

Article

Fecal microbial load is a major determinant of gut microbiome variation and a confounder for disease associations

Graphical abstract

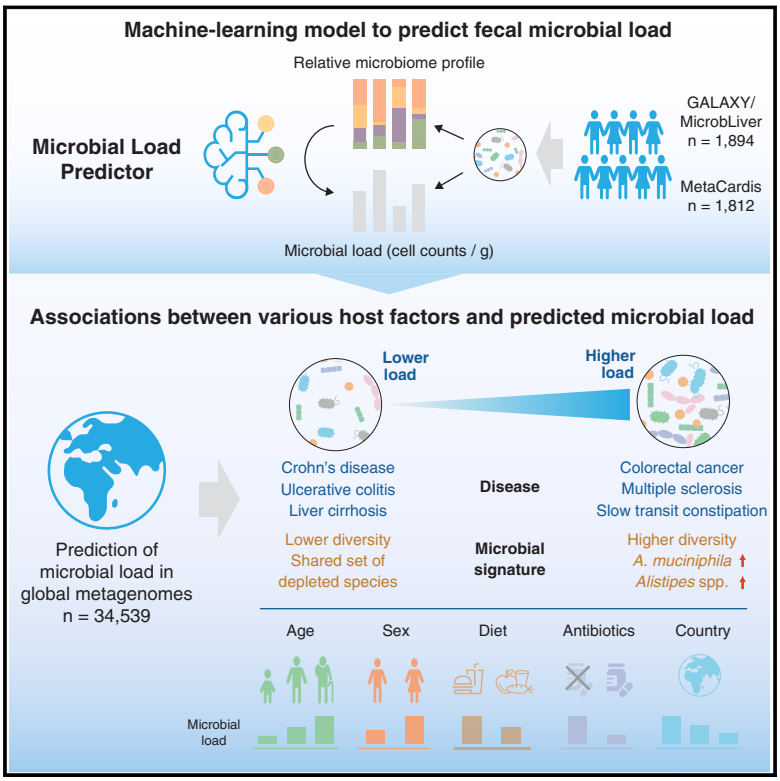

Highlights

- Machine-learning model predicts fecal microbial load from relative microbiome profile
- Predicted loads correlate with host and environmental factors in a large-scale dataset
- Disease-associated microbial signatures are linked to predicted microbial load
- Predicted load adjustment reduces statistical significance of disease-associated species

Authors

Suguru Nishijima, Evelina Stankevic, Oliver Aasmets, ..., Michael Kuhn, Peer Bork, GALAXY and MicrobLiver Consortia

Correspondence

mkuhn@embl.de (M.K.), peer.bork@embl.org (P.B.)

In brief

A machine-learning approach enables the quantification of microbial load (microbial cells per gram) in fecal samples based on the relative microbiome profile. The predicted microbial load emerged as a major determinant of microbiome variation, confounding various disease-microbe associations across more than 34,000 global metagenomes.

Nishijima et al., 2025, Cell *188*, 222–236
January 9, 2025
https://doi.org/10.1016/j.cell.2024.10.022

CellPress

CellPress
OPEN ACCESS

Cell

Article

Fecal microbial load is a major determinant of gut microbiome variation and a confounder for disease associations

Suguru Nishijima,[1] Evelina Stankevic,[2] Oliver Aasmets,[3] Thomas S.B. Schmidt,[1,16] Naoyoshi Nagata,[4] Marisa Isabell Keller,[1] Pamela Ferretti,[1] Helene Bæk Juel,[2] Anthony Fullam,[1] Shahriyar Mahdi Robbani,[1] Christian Schudoma,[1] Johanne Kragh Hansen,[5,6] Louise Aas Holm,[2,7] Mads Israelsen,[5,6] Robert Schierwagen,[8] Nikolaj Torp,[5,6] Anja Telzerow,[1] Rajna Hercog,[1] Stefanie Kandels,[1] Diënty H.M. Hazenbrink,[1] Manimozhiyan Arumugam,[2] Flemming Bendtsen,[9] Charlotte Brøns,[10] Cilius Esmann Fonvig,[2,7,11] Jens-Christian Holm,[2,7,11] Trine Nielsen,[2,11,12] Julie Steen Pedersen,[9] Maja Sofie Thiele,[5,6] Jonel Trebicka,[8,13] Elin Org,[3] Aleksander Krag,[5,6] Torben Hansen,[2] Michael Kuhn,[1,*] Peer Bork,[1,14,15,17,*] and GALAXY and MicrobLiver Consortia

[1]Molecular Systems Biology Unit, European Molecular Biology Laboratory, Heidelberg, Germany
[2]Novo Nordisk Foundation Center for Basic Metabolic Research, University of Copenhagen, Copenhagen, Denmark
[3]Institute of Genomics, University of Tartu, Tartu, Estonia
[4]Department of Gastroenterological Endoscopy, Tokyo Medical University, Tokyo, Japan
[5]Faculty of Health Sciences, University of Southern Denmark, Odense, Denmark
[6]Department of Gastroenterology and Hepatology, Odense University Hospital, Odense, Denmark
[7]The Children's Obesity Clinic, Department of Pediatrics, Copenhagen University Hospital Holbæk, Holbæk, Denmark
[8]Department of Internal Medicine B, University of Münster, Münster, Germany
[9]Gastrounit, Medical Division, Copenhagen University Hospital Hvidovre, Hvidovre, Denmark
[10]Clinical Research, Steno Diabetes Center Copenhagen, Herlev, Denmark
[11]Department of Clinical Medicine, Faculty of Health and Medical Sciences, University of Copenhagen, Copenhagen, Denmark
[12]Medical department, University Hospital Zeeland, Køge, Denmark
[13]European Foundation for the Study of Chronic Liver Failure, EFCLIF, Barcelona, Spain
[14]Max Delbrück Centre for Molecular Medicine, Berlin, Germany
[15]Department of Bioinformatics, Biocenter, University of Würzburg, Würzburg, Germany
[16]Present address: APC Microbiome & School of Medicine, University College Cork, Cork, Ireland
[17]Lead contact
*Correspondence: mkuhn@embl.de (M.K.), peer.bork@embl.org (P.B.)
https://doi.org/10.1016/j.cell.2024.10.022

SUMMARY

The microbiota in individual habitats differ in both relative composition and absolute abundance. While sequencing approaches determine the relative abundances of taxa and genes, they do not provide information on their absolute abundances. Here, we developed a machine-learning approach to predict fecal microbial loads (microbial cells per gram) solely from relative abundance data. Applying our prediction model to a large-scale metagenomic dataset (n = 34,539), we demonstrated that microbial load is the major determinant of gut microbiome variation and is associated with numerous host factors, including age, diet, and medication. We further found that for several diseases, changes in microbial load, rather than the disease condition itself, more strongly explained alterations in patients' gut microbiome. Adjusting for this effect substantially reduced the statistical significance of the majority of disease-associated species. Our analysis reveals that the fecal microbial load is a major confounder in microbiome studies, highlighting its importance for understanding microbiome variation in health and disease.

INTRODUCTION

Shotgun metagenomic sequencing facilitates high-throughput profiling of complex microbial communities in environmental samples.[1–3] Applied to the human gut microbiome, metagenomics reveals its structure, function, and variations[4–6] as well as its associations with host physiologies, including diseases, immune function, and response to cancer therapy.[7–11] However, the microbial profiles obtained from metagenomic analysis are inherently compositional, with the abundance of each microbial species represented in relative proportions (fraction of total reads).[12–14] In such compositional data, changes in one microbial species result in concurrent relative changes in others, leading to negative correlation bias that can cause false positives

and false negatives in association studies.[12,13] Moreover, sequencing data do not provide information on microbial load (i.e., the total number of prokaryotic cells per gram or microbial density), which is closely associated with fecal transit time,[15–17] stool consistency,[18] water content,[19] and pH[20,21] in the gut and is a key ecological factor in shaping the diversity, metabolism, and inter-individual variation of the microbiome.[19,22]

To overcome these issues and to factor in total absolute abundances, various experimental methods are applied to microbiome studies, such as flow cytometry-based cell counting,[19,23,24] quantitative PCR,[25–27] or internal standard provision (e.g., spike-in DNA)[28–31] that quantify the microbial load in environmental samples. Such additional data help avoid pitfalls associated with compositional data[13] and link microbiome variation across individuals with changes in microbial load.[19,32] However, generating such quantitative profiles requires extra experiments that are labor-intensive, costly, and impractical for large-scale microbiome studies. Hence, the vast majority of public or ongoing metagenomic studies do not take into account associated microbial loads in their analyses.

Here, we present a machine-learning model capable of robustly predicting microbial load without requiring additional wet lab assays. Using large-scale paired datasets of metagenomes and microbial load data from two independent study populations (GALAXY/MicrobLiver and MetaCardis), we first train our model to predict the microbial load of a human fecal sample directly from relative microbiome profiles. We then demonstrate the utility of our model by applying it to a large-scale collection of public metagenomic datasets (n = 34,539), revealing significant associations between various host physiologies and predicted microbial load. Furthermore, we show that microbial load is a major determinant of microbiome variation and frequently confounds disease associations of microbial species, with implications for biomarker development.

RESULTS

Microbial load is strongly correlated with taxonomic and functional profiles of the gut microbiome

We based our analysis on fecal samples collected in two independent large-scale study populations by the GALAXY/MicrobLiver (n = 1,894, 46.7 ± 20.3 years old [mean ± SD], males 69.5%) and MetaCardis consortia (n = 1,812, 54.6 ± 13.0 years old [mean ± SD], males 44.8%).[33–35] GALAXY/MicrobLiver encompassed various sub-cohorts, including heterogeneous individuals such as healthy controls, early- to advanced-stage liver disease patients, individuals who participated in intervention trials, and children/adolescents with obesity (see STAR Methods and Tables S1A and S1B). Meanwhile, MetaCardis focused on cardiometabolic disease patients (e.g., coronary artery disease, metabolic syndrome, type 2 diabetes, and severe/morbid obesity) as well as healthy individuals[33–35] (Table S1A). While the data on MetaCardis have been reported elsewhere,[33–35] we present here newly obtained metagenomes and microbial load data from the GALAXY/MicrobLiver consortium (Table S1C). The microbial load of each sample was measured by flow cytometry-based cell counting (see STAR Methods), which provides results that are consistent with qPCR and spike-in DNA.[19,28–30,36] As in many studies, we focused here on the prokaryotic community, which is a major component of the human gut microbiome, and obtained species-level taxonomic and functional (gene) profiles with a marker gene-based method using the mOTUs profiler[37] and the Global Microbial Gene Catalog (GMGC),[38] respectively. The microbial loads in the two study populations were significantly different (mean values were 6.5 ± 2.7e10 and 11.1 ± 5.8e10 for the GALAXY/MicrobLiver and MetaCardis study populations, respectively), suggesting possible study effects due to differences in experimental techniques used to measure load in respective study populations (Figure S1B; see STAR Methods). Nonetheless, taxonomic and functional profiles of the microbiome were consistently associated with the microbial loads in both study populations (Figures S1C and S1D; Tables S2A and S2B).

We first associated the experimentally measured microbial loads with three enterotypes.[39,40] The microbial load was the highest in *Firmicutes* (*Ruminococcus*) enterotype, followed by *Prevotella* and *Bacteroides* enterotypes in both study populations (Figures 1A and 1B). Diversity indexes (e.g., Shannon diversity, species richness, and Simpson diversity) of the microbiome had consistent positive correlations with microbial load, with Shannon diversity showing one of the strongest positive associations in both study populations (Figure 1C). We next studied correlations between relative species abundance and total microbial load and observed positive correlations for various uncultured species in *Firmicutes* phylum, short-chain fatty acid producers,[41] and slow-growing[42] species (e.g., *Oscillibacter*, *Faecalibacterium*, and *Eubacterium* spp.). By contrast, we observed negative correlations for disease-associated species such as *Ruminococcus gnavus* with inflammatory bowel disease[43,44] and *Flavonifractor plautii* with colorectal cancer[45] (Figure 1C; Table S2A). Typical oral species also found in stool, such as *Streptococcus* and *Veillonella* spp., were also negatively associated with microbial load (Figure S1E).

When correlating the microbial loads with the relative functional profiles of the human gut metagenome, we found that microbial genes for lipopolysaccharide (LPS) biosynthesis were enriched in samples with low microbial loads in both study populations (Figure S1F; Table S2B). Similarly, genes for sugar metabolism, including the phosphotransferase system and fructose/mannose metabolism, were consistently associated with lower microbial loads in both study populations. On the other hand, genes involved in flagella assembly and bacterial chemotaxis were positively correlated with the high microbial load in both study populations (Figure S1F). As increased LPS levels in the gut could cause inflammation and diarrhea (i.e., shorter transit time),[46] these genes might also be associated with fecal transit time.

Microbial load is robustly predicted from the taxonomic and functional profiles of the gut microbiome

As we observed strong associations between microbial load and relative gut microbiome profiles, we hypothesized that the microbial load of a fecal sample could be predicted from relative abundances of taxa. We thus trained eXtreme Gradient Boosting

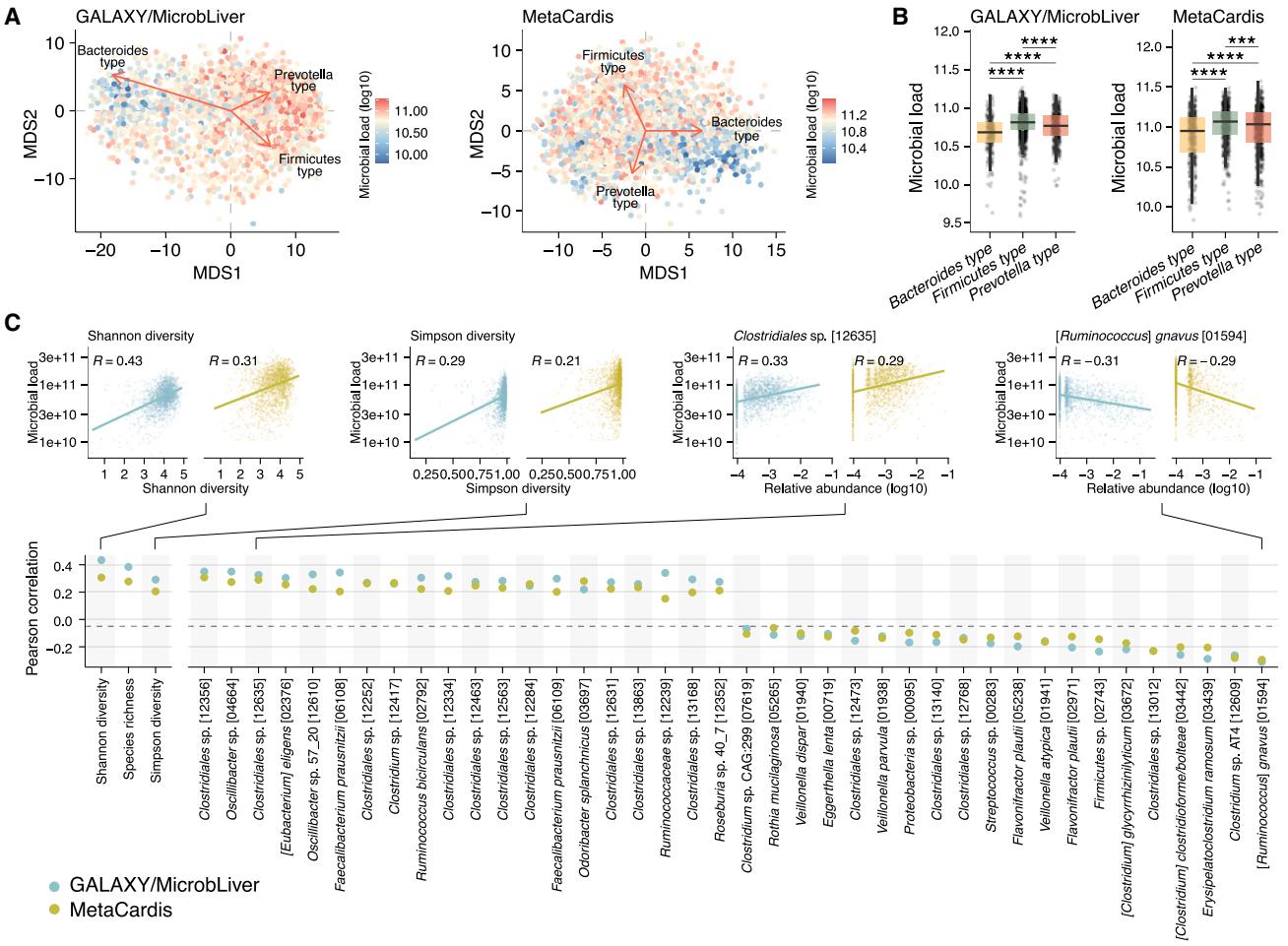

Figure 1. Microbial load is robustly associated with the taxonomic profile of the gut microbiome in the two study populations

(A) Multidimensional scaling plot of the species-level taxonomic profile of the microbiomes in the GALAXY/MicrobLiver (n = 1,894) and MetaCardis (n = 1,812) study populations. Each point represents a sample, and the color shows the $\log_{10}$ transformed microbial load of the sample. Arrows represent the three enterotypes plotted by the envfit function in R. The direction of the arrow indicates the centroid of each enterotype, and the length indicates the strength of the correlation with the enterotype.

(B) Associations between the microbial loads and the enterotypes. Boxplots show the $\log_{10}$-transformed microbial load across the three enterotypes in each cohort. ****$p < 0.0001$, ***$p < 0.001$ (Wilcoxon rank-sum test).

(C) Pearson correlations between microbial load and relative abundances of microbial species (both values were $\log_{10}$ transformed). The three diversity indexes and the top 40 species with the highest correlations are shown. Scatter plots for the two diversity indexes and two microbial species are shown above the heatmap, as examples.

See also Figure S1.

(XGBoost) regression models[47] based on relative abundance of each microbial species as well as the Shannon diversity index (see STAR Methods). Internal 5-times repeated 10-fold cross-validation in each study population showed that both models predicted the microbial load with Pearson correlation coefficients of 0.67 ± 0.0068 and 0.68 ± 0.0069 (mean ± SD) for the GALAXY/MicrobLiver and MetaCardis study populations, respectively (Figure 2A). To evaluate the robustness of the model in an external dataset, we applied each model to the other dataset and found that both models again predicted the microbial loads significantly (Pearson correlation coefficient = 0.56 for both the GALAXY/MicrobLiver and MetaCardis models). Functional profiles at the Kyoto Encyclopedia of Genes and Genomes (KEGG) orthology level also predicted the microbial loads with comparable accuracies to those trained by the species-level taxonomic profiles (Figure 2B). These results demonstrated robust prediction of microbial loads in fecal samples from relative microbiome profiles obtained by metagenomic sequencing.

To further explore the applicability to different sequencing technologies, we collected additional paired data of 16S rRNA gene sequencing and fecal microbial loads from two previous studies[19,24] (see STAR Methods). The internal and external validations of the model between the two studies also demonstrated robust prediction of microbial load (Pearson correlation coefficient = 0.79 for the internal validation and 0.60 for the external validation, Figure 2C), indicating that with sufficient data, fecal

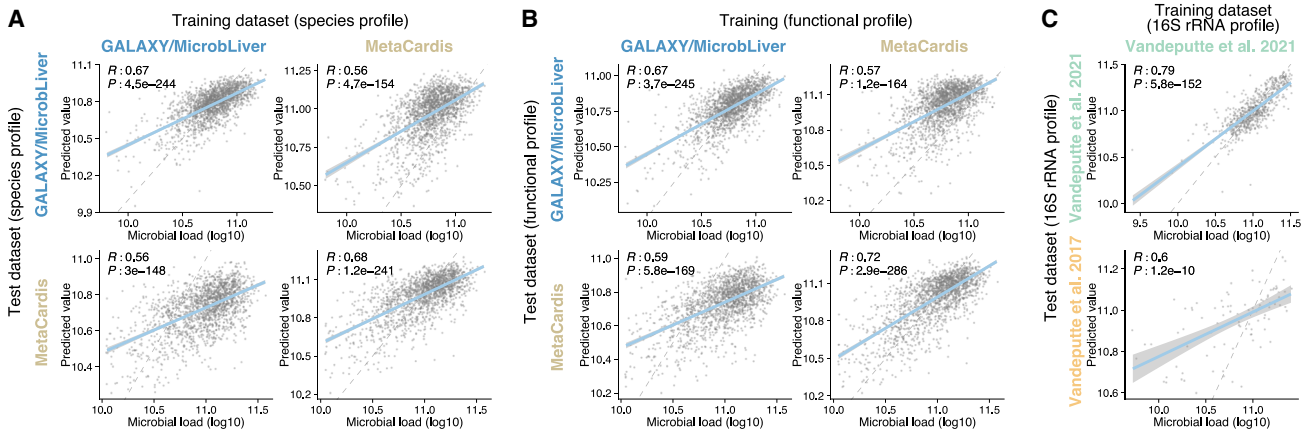

Figure 2. Machine-learning models robustly predict microbial loads of fecal samples

Scatterplots showing the predictive performance of XGBoost regression models for fecal microbial load. The models were trained to predict microbial load based on the species-level taxonomic profile (A), functional profile with the KEGG orthology level (B), and 16S rRNA gene profile (C) of the microbiome. For the species and functional models, the metagenomes of the GALAXY/MicrobLiver (n = 1,894) and MetaCardis (n = 1,812) study populations were used to construct them. These models were internally evaluated with a 5-times repeated 10-fold cross-validation and externally by applying to each other's dataset (i.e., test dataset). For the 16S rRNA gene model, samples from Vandeputte et al.[24] (n = 707) were used to construct. An independent dataset from Vandeputte et al.[19] (n = 95) was employed for the external validation. The solid blue lines show regression lines, and the gray dashed lines represent 1:1 reference lines. Pearson correlations between experimentally measured and predicted microbial loads are shown with p values.
See also Figure S2.

microbial loads can be predicted from different relative abundance measures.

Since the GALAXY/MicrobLiver and MetaCardis study populations included individuals with different phenotypes and demographic factors (e.g., healthy adults, diseased patients, and children/adolescents, Table S1), we next examined how prediction accuracy differed among these groups. Notably, we found that both models robustly predicted microbial load not only in healthy samples but also in diseased samples that were not included in the model's training (Figures S2A and S2B). Specifically, the MetaCardis model, which was trained on samples from healthy adults and cardiometabolic disease patients, showed comparative accuracy among the sub-cohorts in the GALAXY/MicrobLiver study population (Figure S2A), with Pearson correlation coefficient of 0.52 for healthy individuals (GALA-HP), 0.47 for early- to middle-stage liver disease patients (GALA-ALD), 0.62 for advanced-stage liver disease patients (TIPS), and 0.53 for children/adolescents (HOLBAEK). Similarly, the GALAXY/MicrobLiver model also showed comparative accuracies for individuals with various diseases in the MetaCardis dataset, with Pearson correlation coefficients of 0.44 for healthy individuals, 0.43 for patients with coronary artery disease, 0.56 for diabetes, 0.48 for metabolic syndrome, and 0.63 for severe obesity/morbid obesity (Figure S2B). As such, the models robustly predict microbial load even for samples with phenotypes not included in the training data.

To further assess the robustness of our prediction models in regard to variation of various technical and biological factors, we next applied our prediction model to metagenomes derived from the same fecal sample sequenced using the same protocol in different laboratories (i.e., technical replicates) and sequenced using different DNA extraction methods, to longitudinal metagenomes obtained from the same individual, and to metagenomes from different individuals in previous studies (Figure S2C).[48–56] The lowest variation in predicted microbial load was observed between technical replicates (coefficient of variation [CV] = 0.12), followed by between metagenomes with different DNA extraction methods (CV = 0.19) and between longitudinal samples from the same individual (CV = 0.19), and the highest variation was observed between samples from different individuals (CV = 0.36) (Figure S2C). These results indicate that biological variability is greater than technical variability for microbial load and that, therefore, with large sample sizes, associations between microbial load and biological factors can be detected using our prediction model.

Predicted microbial loads are significantly associated with various host factors

To investigate the associations between predicted microbial loads and host factors such as diet, lifestyle, medication, and disease status, we collected public gut metagenomes from 159 previous studies across 45 countries (n = 27,832, 46.3 ± 19.3 years old [mean ± SD], 52.9% males; Tables S3A and S3B). Additionally, we collected metagenomes from two large population studies[57,58]: Japanese 4D cohort (n = 4,198, 66.4 ± 12.6 years old [mean ± SD], 58.8% males) and Estonian Microbiome cohort (n = 2,509, 50.0 ± 14.9 years old [mean ± SD], 29.7% males), in which deep phenotyping was performed and various host and environmental factors were available (Tables S3C and S3D). Since the former data were derived from various smaller studies with less host intrinsic and extrinsic factor information, they were combined into a global dataset. We prepared species-level taxonomic profiles of each sample and predicted microbial load using the MetaCardis prediction model (see STAR Methods and Figure S1). Redundancy analysis showed that the predicted microbial load had the strongest

Figure 3. Predicted microbial loads are associated with various host factors

(A) Predicted microbial loads of the collected metagenomes across different countries. Individuals treated with antibiotics and those with any diseases were excluded. The average microbial loads of the 34 countries with at least 20 individuals are shown.

(B) Comparison of the predicted microbial loads among four groups of countries divided by economic size. Definitions of the groups were obtained from the World Bank. The letters above the boxes (a, b, and c) indicate statistically significant differences ($p < 0.01$) between groups with different letters (Wilcoxon rank-sum test).

(C) Associations between the predicted microbial load and various host factors in the Japanese 4D and Estonian Microbiome cohorts. The explained variances by the host factors (coefficient of determination) were assessed by linear regression models, including these host factors as explanatory variables and the $\log_{10}$ transformed microbial load as a response variable.

(legend continued on next page)

association with the gut microbiome variation among various host and environmental factors, such as diet, lifestyle, disease, and medication, in both the Japanese 4D and Estonian Microbiome cohorts (Figure S3A), indicating a strong interaction between microbial load and gut microbiome composition.

In the global dataset, samples from high-income countries showed significantly higher predicted microbial loads than those from low-income countries (Figures 3A and 3B). This difference could not be attributed to the potential bias that the model was trained on samples from high-income countries (Figure S3B), suggesting that factors associated with increased income such as lifestyle, diet, or hygiene affect the microbial load. In the Japanese 4D and Estonian Microbiome cohorts, the medication category showed the strongest association with the predicted microbial load among the metadata categories (Figure 3C), which was consistent with the strongest impact of medication on the relative gut microbiome profile observed previously.[57] Anthropometric factors and disease status followed in the Japanese 4D cohort, while diet and other factors ranked next in the Estonian Microbiome cohort. Among the available host factors in the Japanese 4D and Estonian Microbiome cohorts, 65 (26.3%) and 8 (3.6%) showed significant associations with the predicted microbial loads, respectively (false discovery rate [FDR] < 0.05, Figure 3D; Tables S3E and S3F). In the three datasets, the self-reported Bristol stool scale (an index that classifies categories of fecal consistency) showed consistent negative correlations with the predicted microbial loads (Figures 3E and S3C). The frequency of defecation, surveyed in the Estonian Microbiome cohort, was also negatively associated with the microbial load (Figure 3F). These results are consistent with findings from previous studies suggesting that fast transit time (e.g., frequent defecation and diarrhea) reduces microbial loads while slow transit time (e.g., infrequent defecation and constipation) increases microbial loads since fecal bacteria grow along the gastrointestinal tract gradually.[18,22] While age was not associated with microbial load in the Estonian Microbiome cohort, it showed significant positive correlations in the Japanese 4D and global datasets (Figure S3D). Overall, elderly individuals (>70 years old) had 9.7% higher microbial load than younger individuals (<30 years old) in the combined datasets (Figure 3G). Sex was consistently associated with the microbial load in all three datasets (Figures 3H and S3E), with women having a 3.5% higher microbial load than men on average. These results are consistent with epidemiological studies that showed slower transit time in elderly people and females.[59,60] Interestingly, elderly individuals and females showed higher microbiome diversity than younger individuals and males, as observed in previous studies,[61,62] while the strength of these associations decreased once adjusted for the effect of the microbial load (Figure S3G). This suggests that the higher microbial load or slower transit time contributes to increased gut microbiome diversity in elderly individuals and females. Other factors significantly associated with microbial load in the Japanese 4D cohort included various medications (e.g., platelet aggregation inhibitors, aminosalicylic acid, and osmotic laxatives), diseases (e.g., Crohn's disease, ulcerative colitis, and HIV infection), diet (e.g., fruits, mushrooms, green tea, and vinegar), and lifestyle (e.g., alcohol consumption) (Figure 3D).

We next examined associations between fecal microbial load and dietary habits, which play a critical role in shaping the gut microbiome.[63–65] When we compared predicted microbial loads among omnivores, vegetarians, and vegans in the global dataset, we found that omnivores had the highest microbial load, followed by vegetarians and vegans (median predicted load = 8.4e10, 7.8e10, and 7.1e10, respectively, Figure 3I). This result aligns with previous research indicating that vegetarian/vegan diets increase the frequency of defecation and softer stools.[66] Additionally, we observed that a high-starch dietary intervention increased predicted microbial load while a low-calorie dietary intervention had no significant effects (Figure S3H), consistent with previous findings that a high-carbohydrate diet is linked to a lower frequency of defecation.[67] Overall, these results indicate that specific dietary habits and components play an important role in shaping microbial load.

Among medications, antibiotics substantially disrupt the microbial community in the human gut,[68,69] but only a few small-scale studies quantified changes in the microbial load.[32,70] As expected, recent antibiotic treatment was negatively associated with predicted microbial loads in all three datasets (Figures 3J and S3F). Using detailed information on classes of antibiotics from the Japanese 4D and Estonian Microbiome cohorts, we found that many classes had significant impact on the microbial loads, such as sulfonamides, third-generation cephalosporins, macrolides, and fluoroquinolone (Figure S3I). We did not find any differences between bactericidal (i.e., those that kill bacteria) and bacteriostatic (i.e., those that prevent bacterial growth) antibiotics, in line with recent findings that there might not be such a clear separation between bactericidal and bacteriostatic groups.[71] To further explore changes in the microbial loads, we focused on two public time-series metagenomic datasets, with data up to 180 days post-antibiotic treatment.[68,69] In one of these,[69] individuals were treated with a combination of three broad-spectrum antibiotics (vancomycin, gentamicin, and meropenem), while in the other,[68] individuals were treated with a second-generation cephalosporin (cefprozil). We found that the predicted microbial loads gradually recovered after the treatment

(D) Associations between the predicted microbial load and each host factor. The explained variance was assessed by linear regression models, and the top 40 factors with the strongest associations in the Japanese 4D cohort (FDR < 0.05) and eight factors with FDR < 0.05 in the Estonian Microbiome cohort are shown in the figure. For visualization, the explained variance for age in the Japanese 4D cohort (2.8%) is plotted above 2.0% on the y axis.

(E–J) Correlations between the predicted microbial load and various host factors, such as the Bristol stool scale (E), gut emptying frequency (F), age (G), sex (H), dietary habits (I), and antibiotics (J) in the combined datasets of the Japanese 4D, Estonian Microbiome, and global datasets. Associations were evaluated with Pearson correlation for (E)–(G) and Wilcoxon rank-sum test for (H)–(J).

(K) Recovery of the predicted microbial load after antibiotic treatment. Boxplot showing the predicted microbial load of each individual at the respective time point. The datasets were collected from Palleja et al. (n = 12) and Raymond et al. (n = 24) studies. Numbers in the plot indicate the p values for comparisons between time points (paired Wilcoxon rank-sum test).

See also Figure S3.

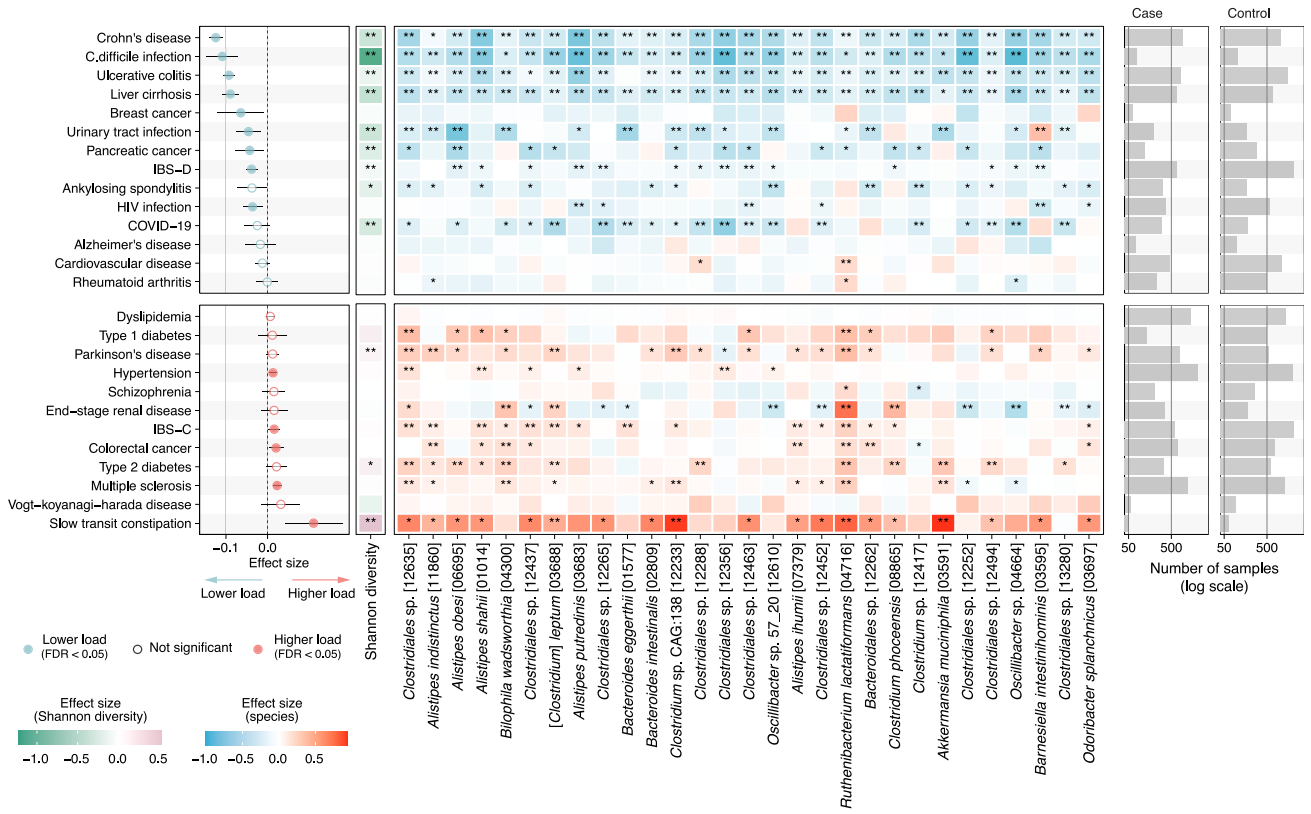

Figure 4. Predicted microbial loads are associated with various diseases

The left forest plot shows the effect sizes of each disease on the predicted microbial load. Blue and red colors represent negative and positive associations with the microbial load compared with the controls, respectively. Filled and empty circles represent significant (FDR < 0.05) and non-significant (FDR > 0.05) associations, respectively. Effect sizes were assessed by a linear regression model including $\log_{10}$ transformed microbial load as a response variable and disease status (i.e., case or control) and each study as explanatory variables. The middle heatmap shows enrichments and depletions of microbial species across different diseases. Blue and red colors represent negative and positive associations, respectively, compared with the controls in each disease dataset. The top 30 species with the strongest differences (FDR < 0.05) in their effect sizes between positively and negatively associated diseases are shown. $^{**}p < 0.01$, $^{*}p < 0.05$ (linear regression analysis). The right bar plot represents the number of samples included in the comparison.

See also Figure S4.

and returned to the baseline level in 180 and 90 days, respectively (Figure 3K). However, the microbial load was still reduced at day 42 following the combinatorial treatment.[69] These results suggest that recovery of microbial load after antibiotic treatments takes at least several weeks. This is consistent with studies on relative species abundances, reporting recovery only after months.[69,72]

Numerous diseases are associated with altered microbial loads

Identification of disease-associated gut species is an important step in developing microbial biomarkers, investigating the etiology of diseases, and developing targeted therapies.[11,73,74] However, the association between microbial load and disease is still largely unexplored, except in a few cases where microbial loads were experimentally determined.[19,32] To evaluate associations between various diseases and the predicted microbial loads, we performed a large-scale case-control analysis by combining the datasets from the global and Japanese 4D datasets, capturing sufficient data for 26 diseases (i.e., >50 cases and controls for each disease) with 13,200 cases and 18,511 controls (Figure S4A; Table S4A). The analysis revealed that the majority of diseases (14/26) were significantly associated with the predicted microbial load (FDR < 0.05). Nine of the significantly associated diseases showed negative associations with the predicted microbial load, while five showed positive associations (Figure 4; Table S4B). The negatively associated diseases included Crohn's disease, ulcerative colitis, liver cirrhosis, *C. difficile* infection, and HIV infection, all of which are frequently associated with diarrhea.[75–77] On average, these patients with these conditions had 17.3% lower predicted microbial loads than controls. Positively associated diseases included slow transit constipation, along with conditions often associated with constipation such as multiple sclerosis, colorectal cancer, and hypertension.[78,79] On average, these patients exhibited 7.7% higher predicted microbial load than the controls. In irritable bowel syndrome (IBS), which is classified into different subtypes according to symptoms, the diarrhea type (IBS-D) showed a significant negative correlation with predicted microbial load (FDR = 3.6e−7), while the constipation

type (IBS-C) showed a significant positive correlation as expected (FDR = 0.042).

To further characterize microbiome profiles in these diseases, we performed a meta-analysis of the relative microbial compositions between cases and controls and defined microbial signatures for each disease based on the coefficient for each species obtained from the regression model (see STAR Methods). Comparison of the signatures between positively and negatively associated diseases revealed a significant difference between the two groups (p = 0.0002, Figure S4B). The majority of the negatively associated diseases were characterized by significantly less diverse microbiomes (e.g., in Crohn's disease, *C. difficile* infection, and ulcerative colitis), which was in line with previous findings that diseases accompanied by diarrhea commonly present reduced microbiome diversity.[80] By contrast, some of the positively associated diseases showed significantly increased microbiome diversity (e.g., slow transit constipation, type 2 diabetes, and Parkinson's disease). Additionally, we identified 86 species that distinguished positively and negatively associated diseases (FDR < 0.05), such as *Alistipes* spp. (*A. putredinis*, *A. indistinctus*, and *A. shahii*), *Bacteroides* spp. (*B. eggerthii*, *B. intestinalis*, and *B. clarus*), and *Eubacterium* spp. (*E. siraeum* and *E.* sp. CAG:202) as well as uncultured *Clostridiales*. The majority of these species were consistently depleted in the patients with negatively associated diseases, while enriched in those with positively associated diseases (Figure 4; Table S4C). These species also included *Bilophila wadsworthia*, a hydrogen sulfide-producing bacteria that may cause systemic inflammation,[81,82] and *Akkermansia muciniphila*, a potential beneficial microbe that may enhance the gut barrier integrity.[83] They have also been identified as slow-growing species in an *in vitro* study,[84] consistent with our observation that they were positively associated with diseases with higher microbial loads (i.e., longer transit time). An unclassified *Burkholderiales* species was the only species consistently enriched in the negatively associated diseases while depleted in positively associated diseases (Table S4C). The presence of these consistent disease-microbe associations across different diseases suggests that some of these disease-associated species are confounded by changes in microbial load.

Microbial load substantially confounds disease-microbe associations

To disentangle species association with disease from those with microbial load in the case-control analyses, we next incorporated predicted microbial load as a covariate in a regression model, which is a method to effectively adjust for such confounding effects in microbiome studies[85,86] (see STAR Methods). We excluded Vogt-Koyanagi-Harada disease and Alzheimer's disease from the following analyses since no significant species were identified in these two diseases (FDR > 0.05). The adjustment led to a considerable reduction in the effect size on the disease-associated species and their statistical significance (in terms of p value) in several diseases. This was especially the case for seven diseases, namely Crohn's disease, ulcerative colitis, liver cirrhosis, IBS-D, breast cancer, *C. difficile* infection, and slow transit constipation (Figure 5). For these conditions, the adjustment led to a decrease in the average effect size by 21.9%–49.9% (35.5% on average, Figure 5A), and consequently, 23.6%–75.0% (48.0% on average) of the previously significant disease-species associations (FDR < 0.05) were no longer significant (FDR > 0.05, Figures 5B and 5C). Of these seven diseases that were particularly affected by the adjustment, six, except for slow transit constipation, were the ones negatively associated with the predicted load. On the other hand, several diseases positively associated with the predicted microbial load, such as end-stage renal disease, colorectal cancer, and multiple sclerosis, showed slight increases in the number of significantly associated species with them (Figure 5C).

Microbial species that lost their significance across different diseases after the adjustment included *Clostridium phoceensis*, *Bacteroides intestinalis*, *Eubacterium eligens*, *Parabacteroides merdae*, and *Faecalibacterium prausnitzii* (Figures 5E and S5A; Table S5), all of which were positively correlated with the experimentally measured microbial load in the GALAXY/MicrobLiver and MetaCardis study populations (Figure 1C; Table S2A). Also, the majority of these species substantially affected by the adjustment were those depleted in the disease patients. These results showed that these bacterial species were more strongly explained by the predicted microbial load than the disease. By contrast, most species significantly enriched in disease patients were not substantially affected by the adjustment. This included *Fusobacterium nucleatum* in colorectal cancer, *Flavonifractor plautii* in Crohn's disease and ulcerative colitis, and *Streptococcus anginosus* in liver cirrhosis and pancreatic cancer (Table S5). Conversely, several enriched species, such as *Erysipelatoclostridium ramosum* and [*Ruminococcus*] *gnavus*, became newly significant after the adjustment in several diseases such as multiple sclerosis and colorectal cancer, respectively (FDR < 0.05, Table S5). These species were significantly enriched in various diseases other than the two diseases, implying that they are involved in pathogenicity[87,88] in a non-disease-specific manner. Additionally, we found that the adjustment decreased the statistical significance of Shannon diversity (Figure 5D), which is one of the most common characteristics to decrease in individuals with diseases,[89,90] in all of the 11 diseases significantly associated with it before the adjustment. In four diseases, such as ulcerative colitis, ankylosing spondylitis, IBS-D, and slow transit constipation, associations with Shannon diversity were not significant after the adjustment (FDR > 0.05). Overall, our results suggest that microbial loads could confound a substantial portion of the results in disease association analyses.

To validate the result of the adjustment based on predicted microbial loads, we further analyzed liver cirrhosis samples (n = 64) from the GALAXY/MicroLiver study and type 2 diabetes samples (n = 539) from the MetaCardis study populations, where both experimentally measured and predicted microbial loads were available. We compared these patient samples with healthy control samples (n = 127 and 275, respectively) to assess the differences in the association between species and disease when using adjustments based on either experimentally determined or predicted loads (Figure S5B). The results showed high consistency in the changes of FDR values for each species due to adjustment, with Pearson correlation coefficients of 0.90 for liver cirrhosis and 0.95 for type 2 diabetes (Figure S5C). Additionally, the statistical significance of Shannon diversity decreased similarly when using both measured and predicted microbial loads

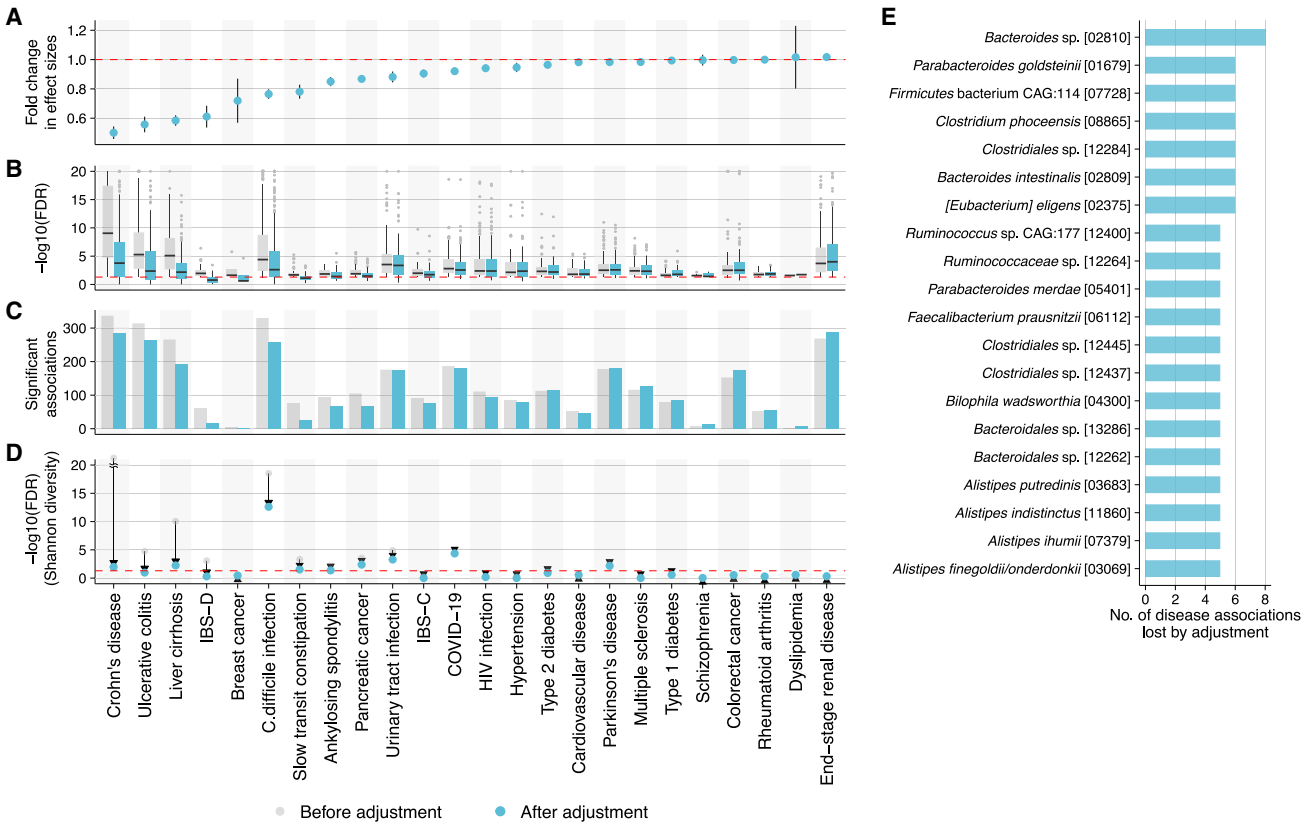

Figure 5. Microbial loads confound disease-microbe associations

(A) Fold change in effect size before and after the adjustment for species that were significantly associated with the disease (FDR < 0.05) before the adjustment for the microbial load. The y axis shows the geometric mean of the ratio of the effect size on the species before and after the adjustment. The error bars show the 95% confidence interval of the geometric mean. Associations between the disease and species abundances were assessed by linear regression analysis with and without the microbial load as a covariate (see STAR Methods). Results for 24 diseases are shown in the plot as Vogt-Koyanagi-Harada disease and Alzheimer's disease had no significant associations with any species (FDR > 0.05).

(B) Comparison of the statistical significance (i.e., FDR) of species before and after the adjustment. For visualization, the maximum on the y axis was set at 20 (i.e., FDR = 1e−20), and extremely lower FDRs were plotted there.

(C) Comparison of the number of significantly associated species (FDR < 0.05) before and after the adjustment.

(D) Comparison of the statistical significance of the Shannon diversity before and after the adjustment. Arrows represent the changes in the FDR before and after the adjustment. Red horizontal line represents FDR = 0.05. For visualization, the FDR for Crohn's disease before adjustment (2.2e−25) is plotted above 20 on the y axis.

(E) The top species (n = 20) that lost their significant associations to at least 5 of the 26 diseases due to the adjustment.

See also Figures S5 and S6.

(Figure S5D). These results show that adjustment based on predicted loads yield results consistent with those based on experimentally measured microbial loads.

Finally, when deriving absolute abundances of microbial species by taking into account the predicted load (i.e., relative abundances multiplied by predicted microbial load), we found that quantitative species profiles reduced biases in relative abundance profiles, therefore reducing over- or underestimation of the significance of species in several diseases associated with microbial load (Figure S6).

DISCUSSION

In this study, we developed machine-learning models to predict microbial load solely based on the relative species and gene abundances of a fecal sample (Figures 1 and 2). The benchmarking (cross-validation within the training cohorts and application to independent study populations) as well as the consistency with existing knowledge on microbial load changes (e.g., after antibiotic treatment) supported the robustness of the prediction. Although various methods are available to experimentally quantify microbial load in fecal samples (e.g., flow cytometry, qPCR, and spike-in DNA), the present models are a convenient way to obtain microbial load without additional wet lab assays, particularly for existing public fecal metagenomes, as it can be directly inferred from relative microbiome profiles.

The application of the prediction models to the large-scale microbiome datasets revealed that predicted microbial load is the major determinant of microbiome variation and various host and environmental factors significantly associated with it, including age, sex, diet, diseases, and medications (Figure 3). Although many of these factors are interdependent, microbial load

appears as a major factor that could explain indirect associations whose mechanisms were unknown (e.g., higher microbial diversity for elderly people and females). These results emphasize the need for analyses that take microbial load into account.

Our analysis also revealed significant differences in microbial loads across various diseases (Figure 4), which indicates that patient microbiomes are not only affected directly by the disease but also indirectly by physiological (e.g., water content, oxygen concentration, and pH) and physical (e.g., transit time) changes that accompany the disease. For example, diarrhea is common in various gastrointestinal and infectious diseases,[91–93] while constipation is a common complication for several neurological diseases such as Parkinson's disease,[94] Alzheimer's disease,[94] and multiple sclerosis,[95] and a risk factor for colorectal cancer.[96] Furthermore, drug treatment could change bowel movement and induce constipation (e.g., opioids, antipsychotics, and non-steroidal anti-inflammatory drugs [NSAIDs]).[97] These observations, along with findings that more than half of the disease-microbe associations lost their significance after the adjustment in several diseases (Figure 5), suggest that microbial load can be a major confounder in disease association studies. This may partly explain the reason why the microbial signatures of a particular disease are often non-specific and shared across multiple diseases, as observed in previous meta-analysis studies.[80,98,99] On the other hand, previous studies have shown that *F. prausnitzii*, which lost significance by the adjustment in several diseases, prevents inflammation (and the resulting decreased transit time).[100] Therefore, the decrease of this species might be the cause of changes in microbial load rather than the result, further necessitating the research to elucidate the causal relationship between them. While our model does not establish causality, it allows for the easy examination of species of interest and their associations with microbial load, which will facilitate the establishment of robust associations between a disease and gut microbes.

The machine-learning model that predicts fecal microbial loads, exclusively based on the relative species abundances, is freely available (MLP, Microbial Load Predictor, https://microbiome-tools.embl.de/mlp/). Although the model was accurate enough to capture known and unknown biological associations, its accuracy will likely increase through refinement with more data or better machine-learning algorithms. In principle, the approach can also be applied to other habitats, making microbial loads comparable, for example, enabling important global studies, such as better estimates of biomass on Earth.

Limitations of the study

While our study demonstrates the utility and robustness of our machine-learning model to predict fecal microbial loads from relative abundance data, several limitations must be acknowledged. Firstly, although the model enables robust prediction, its prediction accuracy was moderate, with correlations ranging from 0.5 to 0.6 in the external validation (Figure 2). This indicates that while the model captures general trends, there is still room for improvement in predicting exact microbial loads in individual samples or small study populations. Additionally, the causal relationship between changes in microbial load and specific gut species remains unclear. Further research is necessary to elucidate whether changes in microbial load drive shifts in species composition or vice versa. Also, the model was developed and validated using fecal samples from children and adults (Table S1), and its applicability to infant and animal fecal samples or biopsy samples is limited. Finally, our analysis primarily focused on the prokaryotic communities and did not consider viruses and eukaryotic microorganisms.

RESOURCE AVAILABILITY

Lead contact

Requests for further information and resources should be directed to and will be fulfilled by the lead contact, Peer Bork (peer.bork@embl.org).

Materials availability

This study did not generate new unique reagents.

Data and code availability

Shotgun metagenomic data sequenced in the GALAXY/MicrobLiver consortia (n = 1,894) are publicly available in the European Nucleotide Archive under the accession number of BioProject: PRJEB76661 (GALA-ALD), BioProject: PRJEB76664 (GALA-HP), BioProject: PRJEB76662 (AlcoChallenge), BioProject: PRJEB76667 (GALA-RIF), BioProject: PRJEB76666 (GastricBypass), BioProject: PRJEB81698 (HCO), BioProject: PRJEB76668 (GALA-POSTBIO), BioProject: PRJEB81697 (HOLBAEK), and BioProject: PRJEB76665 (TIPS). The microbial loads of these fecal samples are available in Table S1C. Metagenomic data of the Estonian Microbiome Cohort is available in the European Genome-Phenome Archive database (EGAS00001008448). The prediction models we constructed (MLP) are available at https://microbiome-tools.embl.de/mlp/ or as R package at https://github.com/grp-bork/microbial_load_predictor/. R codes used to train and construct the prediction models and to generate figures are available at https://github.com/grp-bork/CellCount_Nishijima_2024/.

ACKNOWLEDGMENTS

We thank members of the Bork group at EMBL for their support and constructive discussions. We also thank Anna Głazek, Anna Schwarz, Roman Thielemann, Leonie Thomas, Ela Cetin, Moritz von Stetten, Mariam Hassen, and Kasimir Noack for their help with the metadata curation. This work was supported by funding from the European Union's Horizon 2020 research and innovation program under grant agreement numbers 668031 (GALAXY) and 825694 (MICROB-PREDICT). This reflects only the authors' view, and the European Commission is not responsible for any use that may be made of the information it contains. The study was also supported by the Novo Nordisk Foundation through a Challenge Grant "MicrobLiver" (grant number NNF15OC0016692) and through a core grant (grant number NNF18CC0034900), the Innovation Fund Denmark (grant number: 0603-00484B), the EMBO Installation Grant (no. 3573), an Estonian Research Council grant (PRG1414), and the Deutsche Forschungsgemeinschaft (DFG, German Research Foundation) under project numbers 460129525 and 403224013 (project A09). S.N. was partially supported by the Overseas Postdoctoral Fellowships of the Uehara Memorial Foundation. C.E.F. was supported by the BRIDGE – Translational Excellence Programme (grant number: NNF18SA0034956), Steno Diabetes Center Sjaelland, and The Region Zealand Health Scientific Research Foundation. N.N. was partially supported by the Japan Agency for Medical Research and Development (AMED) (Research Program on HIV/AIDS: JP22fk0410051 and Research Program on Emerging and Re-emerging Infectious Diseases: JP22fk0108538) and the Ministry of Health, Labour, and Welfare, Japan (grant number: 22HB1003). L.A.H. was supported by the Danish Cardiovascular Academy, which is funded by the Novo Nordisk Foundation (grant no. NNF20SA0067242) and the Danish Heart Foundation (grant no. PhD2023009-HF).

AUTHOR CONTRIBUTIONS

Conceptualization, S.N., M.K., and P.B.; methodology, S.N.; data analysis, S.N., O.A., M.I.K., A.F., C.S., and S.M.R.; sample collection, J.K.H., L.A.H.,

M.I., R.S., N.T., M.A., F.B., C.B., C.E.F., J.-C.H., T.N., J.S.P., M.S.T., J.T., N.N., E.O., and A.K.; sequencing, A.T., R.H., S.K., and D.H.M.H.; cell counting, E.S., H.B.J., and T.H.; collection of public metagenomes and metadata curation, T.S.B.S., P.F., S.N., A.F., and M.K.; writing, S.N., M.K., and P.B.; supervision, J.T., E.O., A.K., T.H., M.K., and P.B. All authors discussed the results, reviewed the manuscript, and approved the final manuscript.

DECLARATION OF INTERESTS

The authors declare no competing interests.

STAR★METHODS

Detailed methods are provided in the online version of this paper and include the following:

- KEY RESOURCES TABLE
- EXPERIMENTAL MODEL AND STUDY PARTICIPANT DETAILS
  - GALAXY/MicrobLiver study population
  - GALA-ALD
  - GALA-HP
  - GALA-RIF
  - AlcoChallenge
  - HCO
  - GALA-POSTBIO
  - GastricBypass
  - The HOLBAEK Study
  - TIPS
- METHOD DETAILS
  - DNA sequencing of fecal samples
  - Quality control of sequenced reads
  - Cell counting
  - Taxonomic and functional profiling of metagenomes
  - MetaCardis dataset
- QUANTIFICATION AND STATISTICAL ANALYSIS
  - Association analysis between the gut microbiome and microbial loads
  - Construction of prediction models
  - Analysis of 16S rRNA gene data from previous studies
  - Collection of external microbiome datasets
  - Evaluation of the effects of biological and technological factors on predicted microbial loads
  - Analysis of the external metagenomic datasets
  - Association analysis between diseases and the microbial load
  - Association analysis between diseases and the microbiome composition
  - Comparison of adjustment based on experimentally measured and predicted microbial loads
  - Comparison of quantitative and relative microbiome profiles in disease association analysis

SUPPLEMENTAL INFORMATION

Supplemental information can be found online at https://doi.org/10.1016/j.cell.2024.10.022.

Received: March 8, 2024
Revised: July 12, 2024
Accepted: October 14, 2024
Published: November 13, 2024

REFERENCES

1. Quince, C., Walker, A.W., Simpson, J.T., Loman, N.J., and Segata, N. (2017). Shotgun metagenomics, from sampling to analysis. Nat. Biotechnol. *35*, 833–844. https://doi.org/10.1038/nbt.3935.
2. Knight, R., Vrbanac, A., Taylor, B.C., Aksenov, A., Callewaert, C., Debelius, J., Gonzalez, A., Kosciolek, T., McCall, L.-I., McDonald, D., et al. (2018). Best practices for analysing microbiomes. Nat. Rev. Microbiol. *16*, 410–422. https://doi.org/10.1038/s41579-018-0029-9.
3. Wooley, J.C., Godzik, A., and Friedberg, I. (2010). A primer on metagenomics. PLOS Comput. Biol. *6*, e1000667. https://doi.org/10.1371/journal.pcbi.1000667.
4. Sommer, F., Anderson, J.M., Bharti, R., Raes, J., and Rosenstiel, P. (2017). The resilience of the intestinal microbiota influences health and disease. Nat. Rev. Microbiol. *15*, 630–638. https://doi.org/10.1038/nrmicro.2017.58.
5. Gilbert, J.A., Blaser, M.J., Caporaso, J.G., Jansson, J.K., Lynch, S.V., and Knight, R. (2018). Current understanding of the human microbiome. Nat. Med. *24*, 392–400. https://doi.org/10.1038/nm.4517.
6. Schmidt, T.S.B., Raes, J., and Bork, P. (2018). The human gut microbiome: from association to modulation. Cell *172*, 1198–1215. https://doi.org/10.1016/j.cell.2018.02.044.
7. Rooks, M.G., and Garrett, W.S. (2016). Gut microbiota, metabolites and host immunity. Nat. Rev. Immunol. *16*, 341–352. https://doi.org/10.1038/nri.2016.42.
8. Honda, K., and Littman, D.R. (2016). The microbiota in adaptive immune homeostasis and disease. Nature *535*, 75–84. https://doi.org/10.1038/nature18848.
9. Levy, M., Kolodziejczyk, A.A., Thaiss, C.A., and Elinav, E. (2017). Dysbiosis and the immune system. Nat. Rev. Immunol. *17*, 219–232. https://doi.org/10.1038/nri.2017.7.
10. Helmink, B.A., Khan, M.A.W., Hermann, A., Gopalakrishnan, V., and Wargo, J.A. (2019). The microbiome, cancer, and cancer therapy. Nat. Med. *25*, 377–388. https://doi.org/10.1038/s41591-019-0377-7.
11. Fan, Y., and Pedersen, O. (2021). Gut microbiota in human metabolic health and disease. Nat. Rev. Microbiol. *19*, 55–71. https://doi.org/10.1038/s41579-020-0433-9.
12. Gloor, G.B., Macklaim, J.M., Pawlowsky-Glahn, V., and Egozcue, J.J. (2017). Microbiome datasets are compositional: and this is not optional. Front. Microbiol. *8*, 2224. https://doi.org/10.3389/fmicb.2017.02224.
13. Lloréns-Rico, V., Vieira-Silva, S., Gonçalves, P.J., Falony, G., and Raes, J. (2021). Benchmarking microbiome transformations favors experimental quantitative approaches to address compositionality and sampling depth biases. Nat. Commun. *12*, 3562. https://doi.org/10.1038/s41467-021-23821-6.
14. Gloor, G.B., Wu, J.R., Pawlowsky-Glahn, V., and Egozcue, J.J. (2016). It's all relative: analyzing microbiome data as compositions. Ann. Epidemiol. *26*, 322–329. https://doi.org/10.1016/j.annepidem.2016.03.003.
15. Roager, H.M., Hansen, L.B.S., Bahl, M.I., Frandsen, H.L., Carvalho, V., Gøbel, R.J., Dalgaard, M.D., Plichta, D.R., Sparholt, M.H., Vestergaard, H., et al. (2016). Colonic transit time is related to bacterial metabolism and mucosal turnover in the gut. Nat. Microbiol. *1*, 1–9. https://doi.org/10.1038/nmicrobiol.2016.93.
16. Asnicar, F., Leeming, E.R., Dimidi, E., Mazidi, M., Franks, P.W., Al Khatib, H., Valdes, A.M., Davies, R., Bakker, E., Francis, L., et al. (2021). Blue poo: impact of gut transit time on the gut microbiome using a novel marker. Gut *70*, 1665–1674. https://doi.org/10.1136/gutjnl-2020-323877.
17. Boekhorst, J., Venlet, N., Procházková, N., Hansen, M.L., Lieberoth, C.B., Bahl, M.I., Lauritzen, L., Pedersen, O., Licht, T.R., Kleerebezem, M., et al. (2022). Stool energy density is positively correlated to intestinal transit time and related to microbial enterotypes. Microbiome *10*, 223. https://doi.org/10.1186/s40168-022-01418-5.
18. Vandeputte, D., Falony, G., Vieira-Silva, S., Tito, R.Y., Joossens, M., and Raes, J. (2016). Stool consistency is strongly associated with gut microbiota richness and composition, enterotypes and bacterial growth rates. Gut *65*, 57–62. https://doi.org/10.1136/gutjnl-2015-309618.
19. Vandeputte, D., Kathagen, G., D'hoe, K., Vieira-Silva, S., Valles-Colomer, M., Sabino, J., Wang, J., Tito, R.Y., De Commer, L., Darzi, Y., et al. (2017).

Quantitative microbiome profiling links gut community variation to microbial load. Nature *551*, 507–511. https://doi.org/10.1038/nature24460.

20. Lewis, S.J., and Heaton, K.W. (1997). Increasing butyrate concentration in the distal colon by accelerating intestinal transit. Gut *41*, 245–251. https://doi.org/10.1136/gut.41.2.245.
21. Ringel-Kulka, T., Choi, C.H., Temas, D., Kim, A., Maier, D.M., Scott, K., Galanko, J.A., and Ringel, Y. (2015). Altered colonic bacterial fermentation as a potential pathophysiological factor in irritable bowel syndrome. Am. J. Gastroenterol. *110*, 1339–1346. https://doi.org/10.1038/ajg.2015.220.
22. Procházková, N., Falony, G., Dragsted, L.O., Licht, T.R., Raes, J., and Roager, H.M. (2023). Advancing human gut microbiota research by considering gut transit time. Gut *72*, 180–191. https://doi.org/10.1136/gutjnl-2022-328166.
23. Props, R., Kerckhof, F.-M., Rubbens, P., De Vrieze, J., Hernandez Sanabria, E., Waegeman, W., Monsieurs, P., Hammes, F., and Boon, N. (2017). Absolute quantification of microbial taxon abundances. ISME J. *11*, 584–587. https://doi.org/10.1038/ismej.2016.117.
24. Vandeputte, D., De Commer, L., Tito, R.Y., Kathagen, G., Sabino, J., Vermeire, S., Faust, K., and Raes, J. (2021). Temporal variability in quantitative human gut microbiome profiles and implications for clinical research. Nat. Commun. *12*, 6740. https://doi.org/10.1038/s41467-021-27098-7.
25. Jian, C., Luukkonen, P., Yki-Järvinen, H., Salonen, A., and Korpela, K. (2020). Quantitative PCR provides a simple and accessible method for quantitative microbiota profiling. PLoS One *15*, e0227285. https://doi.org/10.1371/journal.pone.0227285.
26. Barlow, J.T., Bogatyrev, S.R., and Ismagilov, R.F. (2020). Publisher Correction: A quantitative sequencing framework for absolute abundance measurements of mucosal and lumenal microbial communities. Nat. Commun. *11*, 3438. https://doi.org/10.1038/s41467-020-17055-1.
27. Maghini, D.G., Dvorak, M., Dahlen, A., Roos, M., Kuersten, S., and Bhatt, A.S. (2023). Quantifying bias introduced by sample collection in relative and absolute microbiome measurements. Nat. Biotechnol. *42*, 328–338.
28. Stämmler, F., Gläsner, J., Hiergeist, A., Holler, E., Weber, D., Oefner, P.J., Gessner, A., and Spang, R. (2016). Adjusting microbiome profiles for differences in microbial load by spike-in bacteria. Microbiome *4*, 28. https://doi.org/10.1186/s40168-016-0175-0.
29. Tourlousse, D.M., Yoshiike, S., Ohashi, A., Matsukura, S., Noda, N., and Sekiguchi, Y. (2017). Synthetic spike-in standards for high-throughput 16S rRNA gene amplicon sequencing. Nucleic Acids Res. *45*, e23. https://doi.org/10.1093/nar/gkw984.
30. Rao, C., Coyte, K.Z., Bainter, W., Geha, R.S., Martin, C.R., and Rakoff-Nahoum, S. (2021). Multi-kingdom ecological drivers of microbiota assembly in preterm infants. Nature *591*, 633–638. https://doi.org/10.1038/s41586-021-03241-8.
31. Tkacz, A., Hortala, M., and Poole, P.S. (2018). Absolute quantitation of microbiota abundance in environmental samples. Microbiome *6*, 110. https://doi.org/10.1186/s40168-018-0491-7.
32. Contijoch, E.J., Britton, G.J., Yang, C., Mogno, I., Li, Z., Ng, R., Llewellyn, S.R., Hira, S., Johnson, C., Rabinowitz, K.M., et al. (2019). Gut microbiota density influences host physiology and is shaped by host and microbial factors. eLife *8*, e40553. https://doi.org/10.7554/eLife.40553.
33. Vieira-Silva, S., Falony, G., Belda, E., Nielsen, T., Aron-Wisnewsky, J., Chakaroun, R., Forslund, S.K., Assmann, K., Valles-Colomer, M., Nguyen, T.T.D., et al. (2020). Statin therapy is associated with lower prevalence of gut microbiota dysbiosis. Nature *581*, 310–315. https://doi.org/10.1038/s41586-020-2269-x.
34. Forslund, S.K., Chakaroun, R., Zimmermann-Kogadeeva, M., Markó, L., Aron-Wisnewsky, J., Nielsen, T., Moitinho-Silva, L., Schmidt, T.S.B., Falony, G., Vieira-Silva, S., et al. (2021). Combinatorial, additive and dose-dependent drug–microbiome associations. Nature *600*, 500–505. https://doi.org/10.1038/s41586-021-04177-9.
35. Fromentin, S., Forslund, S.K., Chechi, K., Aron-Wisnewsky, J., Chakaroun, R., Nielsen, T., Tremaroli, V., Ji, B., Prifti, E., Myridakis, A., et al. (2022). Microbiome and metabolome features of the cardiometabolic disease spectrum. Nat. Med. *28*, 303–314. https://doi.org/10.1038/s41591-022-01688-4.
36. Galazzo, G., van Best, N., Benedikter, B.J., Janssen, K., Bervoets, L., Driessen, C., Oomen, M., Lucchesi, M., van Eijck, P.H., Becker, H.E.F., et al. (2020). How to Count Our microbes? The effect of different quantitative microbiome profiling approaches. Front. Cell. Infect. Microbiol. *10*, 403. https://doi.org/10.3389/fcimb.2020.00403.
37. Milanese, A., Mende, D.R., Paoli, L., Salazar, G., Ruscheweyh, H.-J., Cuenca, M., Hingamp, P., Alves, R., Costea, P.I., Coelho, L.P., et al. (2019). Microbial abundance, activity and population genomic profiling with mOTUs2. Nat. Commun. *10*, 1014. https://doi.org/10.1038/s41467-019-08844-4.
38. Coelho, L.P., Alves, R., del Río, Á.R., Myers, P.N., Cantalapiedra, C.P., Giner-Lamia, J., Schmidt, T.S., Mende, D.R., Orakov, A., Letunic, I., et al. (2022). Towards the biogeography of prokaryotic genes. Nature *601*, 252–256. https://doi.org/10.1038/s41586-021-04233-4.
39. Arumugam, M., Raes, J., Pelletier, E., Le Paslier, D., Yamada, T., Mende, D.R., Fernandes, G.R., Tap, J., Bruls, T., Batto, J.-M., et al. (2011). Enterotypes of the human gut microbiome. Nature *473*, 174–180. https://doi.org/10.1038/nature09944.
40. Costea, P.I., Hildebrand, F., Arumugam, M., Bäckhed, F., Blaser, M.J., Bushman, F.D., de Vos, W.M., Ehrlich, S.D., Fraser, C.M., Hattori, M., et al. (2018). Enterotypes in the landscape of gut microbial community composition. Nat. Microbiol. *3*, 8–16. https://doi.org/10.1038/s41564-017-0072-8.
41. Louis, P., and Flint, H.J. (2009). Diversity, metabolism and microbial ecology of butyrate-producing bacteria from the human large intestine. FEMS Microbiol. Lett. *294*, 1–8. https://doi.org/10.1111/j.1574-6968.2009.01514.x.
42. Adamberg, K., and Adamberg, S. (2018). Selection of fast and slow growing bacteria from fecal microbiota using continuous culture with changing dilution rate. Microb. Ecol. Health Dis. *29*, 1549922. https://doi.org/10.1080/16512235.2018.1549922.
43. Hall, A.B., Yassour, M., Sauk, J., Garner, A., Jiang, X., Arthur, T., Lagoudas, G.K., Vatanen, T., Fornelos, N., Wilson, R., et al. (2017). A novel Ruminococcus gnavus clade enriched in inflammatory bowel disease patients. Genome Med. *9*, 103. https://doi.org/10.1186/s13073-017-0490-5.
44. Henke, M.T., Kenny, D.J., Cassilly, C.D., Vlamakis, H., Xavier, R.J., and Clardy, J. (2019). Ruminococcus gnavus, a member of the human gut microbiome associated with Crohn's disease, produces an inflammatory polysaccharide. Proc. Natl. Acad. Sci. USA *116*, 12672–12677. https://doi.org/10.1073/pnas.1904099116.
45. Gupta, A., Dhakan, D.B., Maji, A., Saxena, R., P K, V.P., Mahajan, S., Pulikkan, J., Kurian, J., Gomez, A.M., Scaria, J., et al. (2019). Association of Flavonifractor plautii, a flavonoid-degrading bacterium, with the gut microbiome of colorectal cancer patients in India. mSystems *4*, e00438-19. https://doi.org/10.1128/mSystems.00438-19.
46. Yang, J., Zhao, Y., and Shao, F. (2015). Non-canonical activation of inflammatory caspases by cytosolic LPS in innate immunity. Curr. Opin. Immunol. *32*, 78–83. https://doi.org/10.1016/j.coi.2015.01.007.
47. Chen, T., and Guestrin, C. (2016). XGBoost: A scalable tree boosting system. In Proceedings of the 22nd ACM SIGKDD International Conference on Knowledge Discovery and Data Mining KDD '16 (Association for Computing Machinery), pp. 785–794. https://doi.org/10.1145/2939672.2939785.
48. Tourlousse, D.M., Narita, K., Miura, T., Sakamoto, M., Ohashi, A., Shiina, K., Matsuda, M., Miura, D., Shimamura, M., Ohyama, Y., et al. (2021). Validation and standardization of DNA extraction and library construction methods for metagenomics-based human fecal microbiome measurements. Microbiome *9*, 95. https://doi.org/10.1186/s40168-021-01048-3.
49. Costea, P.I., Zeller, G., Sunagawa, S., Pelletier, E., Alberti, A., Levenez, F., Tramontano, M., Driessen, M., Hercog, R., Jung, F.-E., et al. (2017).

Towards standards for human fecal sample processing in metagenomic studies. Nat. Biotechnol. *35*, 1069–1076. https://doi.org/10.1038/nbt.3960.

50. Zeevi, D., Korem, T., Zmora, N., Israeli, D., Rothschild, D., Weinberger, A., Ben-Yacov, O., Lador, D., Avnit-Sagi, T., Lotan-Pompan, M., et al. (2015). Personalized nutrition by prediction of glycemic responses. Cell *163*, 1079–1094. https://doi.org/10.1016/j.cell.2015.11.001.
51. Mehta, R.S., Abu-Ali, G.S., Drew, D.A., Lloyd-Price, J., Subramanian, A., Lochhead, P., Joshi, A.D., Ivey, K.L., Khalili, H., Brown, G.T., et al. (2018). Stability of the human faecal microbiome in a cohort of adult men. Nat. Microbiol. *3*, 347–355. https://doi.org/10.1038/s41564-017-0096-0.
52. Hansen, L.B.S., Roager, H.M., Søndertoft, N.B., Gøbel, R.J., Kristensen, M., Vallès-Colomer, M., Vieira-Silva, S., Ibrügger, S., Lind, M.V., Mærkedahl, R.B., et al. (2018). A low-gluten diet induces changes in the intestinal microbiome of healthy Danish adults. Nat. Commun. *9*, 4630. https://doi.org/10.1038/s41467-018-07019-x.
53. Lloyd-Price, J., Arze, C., Ananthakrishnan, A.N., Schirmer, M., Avila-Pacheco, J., Poon, T.W., Andrews, E., Ajami, N.J., Bonham, K.S., Brislawn, C.J., et al. (2019). Multi-omics of the gut microbial ecosystem in inflammatory bowel diseases. Nature *569*, 655–662. https://doi.org/10.1038/s41586-019-1237-9.
54. Poole, A.C., Goodrich, J.K., Youngblut, N.D., Luque, G.G., Ruaud, A., Sutter, J.L., Waters, J.L., Shi, Q., El-Hadidi, M., Johnson, L.M., et al. (2019). Human salivary amylase gene copy number impacts oral and gut microbiomes. Cell Host Microbe *25*, 553–564.e7. https://doi.org/10.1016/j.chom.2019.03.001.
55. Mars, R.A.T., Yang, Y., Ward, T., Houtti, M., Priya, S., Lekatz, H.R., Tang, X., Sun, Z., Kalari, K.R., Korem, T., et al. (2020). Longitudinal multi-omics reveals subset-specific mechanisms underlying irritable bowel syndrome. Cell *182*, 1460–1473.e17. https://doi.org/10.1016/j.cell.2020.08.007.
56. Odenwald, M.A., Lin, H., Lehmann, C., Dylla, N.P., Cole, C.G., Mostad, J.D., Pappas, T.E., Ramaswamy, R., Moran, A., Hutchison, A.L., et al. (2023). Bifidobacteria metabolize lactulose to optimize gut metabolites and prevent systemic infection in patients with liver disease. Nat. Microbiol. *8*, 2033–2049. https://doi.org/10.1038/s41564-023-01493-w.
57. Nagata, N., Nishijima, S., Miyoshi-Akiyama, T., Kojima, Y., Kimura, M., Aoki, R., Ohsugi, M., Ueki, K., Miki, K., Iwata, E., et al. (2022). Population-level metagenomics uncovers distinct effects of multiple medications on the human gut microbiome. Gastroenterology *163*, 1038–1052. https://doi.org/10.1053/j.gastro.2022.06.070.
58. Aasmets, O., Krigul, K.L., Lüll, K., Metspalu, A., and Org, E. (2022). Gut metagenome associations with extensive digital health data in a volunteer-based Estonian microbiome cohort. Nat. Commun. *13*, 869. https://doi.org/10.1038/s41467-022-28464-9.
59. Degen, L.P., and Phillips, S.F. (1996). Variability of gastrointestinal transit in healthy women and men. Gut *39*, 299–305. https://doi.org/10.1136/gut.39.2.299.
60. Madsen, J.L., and Graff, J. (2004). Effects of ageing on gastrointestinal motor function. Age Ageing *33*, 154–159. https://doi.org/10.1093/ageing/afh040.
61. Odamaki, T., Kato, K., Sugahara, H., Hashikura, N., Takahashi, S., Xiao, J.-Z., Abe, F., and Osawa, R. (2016). Age-related changes in gut microbiota composition from newborn to centenarian: a cross-sectional study. BMC Microbiol. *16*, 90. https://doi.org/10.1186/s12866-016-0708-5.
62. Jacobo, C.Z., Kelley Scott, T., Yingfeng, C., Escobar Juan, S., Mueller Noel, T., Ley Ruth, E., McDonald, D., Huang, S., Swafford Austin, D., Knight, R., et al. (2019). Age- and Sex-Dependent Patterns of Gut Microbial Diversity in Human Adults. mSystems *4*, e00261-19. https://doi.org/10.1128/msystems.00261–19.
63. Bisanz, J.E., Upadhyay, V., Turnbaugh, J.A., Ly, K., and Turnbaugh, P.J. (2019). Meta-analysis reveals reproducible gut microbiome alterations in response to a high-fat diet. Cell Host Microbe *26*, 265–272.e4. https://doi.org/10.1016/j.chom.2019.06.013.
64. Bolte, L.A., Vich Vila, A., Imhann, F., Collij, V., Gacesa, R., Peters, V., Wijmenga, C., Kurilshikov, A., Campmans-Kuijpers, M.J.E., Fu, J., et al. (2021). Long-term dietary patterns are associated with pro-inflammatory and anti-inflammatory features of the gut microbiome. Gut *70*, 1287–1298. https://doi.org/10.1136/gutjnl-2020-322670.
65. Asnicar, F., Berry, S.E., Valdes, A.M., Nguyen, L.H., Piccinno, G., Drew, D.A., Leeming, E., Gibson, R., Le Roy, C., Khatib, H.A., et al. (2021). Microbiome connections with host metabolism and habitual diet from 1,098 deeply phenotyped individuals. Nat. Med. *27*, 321–332. https://doi.org/10.1038/s41591-020-01183-8.
66. Davies, G.J., Crowder, M., Reid, B., and Dickerson, J.W. (1986). Bowel function measurements of individuals with different eating patterns. Gut *27*, 164–169. https://doi.org/10.1136/gut.27.2.164.
67. Brinkworth, G.D., Noakes, M., Clifton, P.M., and Bird, A.R. (2009). Comparative effects of very low-carbohydrate, high-fat and high-carbohydrate, low-fat weight-loss diets on bowel habit and faecal short-chain fatty acids and bacterial populations. Br. J. Nutr. *101*, 1493–1502. https://doi.org/10.1017/S0007114508094658.
68. Raymond, F., Ouameur, A.A., Déraspe, M., Iqbal, N., Gingras, H., Dridi, B., Leprohon, P., Plante, P.-L., Giroux, R., Bérubé, È., et al. (2016). The initial state of the human gut microbiome determines its reshaping by antibiotics. ISME J. *10*, 707–720. https://doi.org/10.1038/ismej.2015.148.
69. Palleja, A., Mikkelsen, K.H., Forslund, S.K., Kashani, A., Allin, K.H., Nielsen, T., Hansen, T.H., Liang, S., Feng, Q., Zhang, C., et al. (2018). Recovery of gut microbiota of healthy adults following antibiotic exposure. Nat. Microbiol. *3*, 1255–1265. https://doi.org/10.1038/s41564-018-0257-9.
70. Hildebrand, F., Moitinho-Silva, L., Blasche, S., Jahn, M.T., Gossmann, T.I., Huerta-Cepas, J., Hercog, R., Luetge, M., Bahram, M., Pryszlak, A., et al. (2019). Antibiotics-induced monodominance of a novel gut bacterial order. Gut *68*, 1781–1790. https://doi.org/10.1136/gutjnl-2018-317715.
71. Maier, L., Goemans, C.V., Wirbel, J., Kuhn, M., Eberl, C., Pruteanu, M., Müller, P., Garcia-Santamarina, S., Cacace, E., Zhang, B., et al. (2021). Unravelling the collateral damage of antibiotics on gut bacteria. Nature *599*, 120–124. https://doi.org/10.1038/s41586-021-03986-2.
72. Voigt, A.Y., Costea, P.I., Kultima, J.R., Li, S.S., Zeller, G., Sunagawa, S., and Bork, P. (2015). Temporal and technical variability of human gut metagenomes. Genome Biol. *16*, 73. https://doi.org/10.1186/s13059-015-0639-8.
73. Wang, J., and Jia, H. (2016). Metagenome-wide association studies: fine-mining the microbiome. Nat. Rev. Microbiol. *14*, 508–522. https://doi.org/10.1038/nrmicro.2016.83.
74. Ratiner, K., Ciocan, D., Abdeen, S.K., and Elinav, E. (2023). Utilization of the microbiome in personalized medicine. Nat. Rev. Microbiol. *22*, 291–308.
75. Yu, Y.R., and Rodriguez, J.R. (2017). Clinical presentation of Crohn's, ulcerative colitis, and indeterminate colitis: symptoms, extraintestinal manifestations, and disease phenotypes. Semin. Pediatr. Surg. *26*, 349–355. https://doi.org/10.1053/j.sempedsurg.2017.10.003.
76. Knox, T.A., Spiegelman, D., Skinner, S.C., and Gorbach, S. (2000). Diarrhea and abnormalities of gastrointestinal function in a cohort of men and women with HIV infection. Am. J. Gastroenterol. *95*, 3482–3489. https://doi.org/10.1111/j.1572-0241.2000.03365.x.
77. Kalaitzakis, E. (2014). Gastrointestinal dysfunction in liver cirrhosis. World J. Gastroenterol. *20*, 14686–14695. https://doi.org/10.3748/wjg.v20.i40.14686.
78. Sonnenberg, A., and Müller, A.D. (1993). Constipation and cathartics as risk factors of colorectal cancer: a meta-analysis. Pharmacology *47*, 224–233. https://doi.org/10.1159/000139862.
79. Ishiyama, Y., Hoshide, S., Mizuno, H., and Kario, K. (2019). Constipation-induced pressor effects as triggers for cardiovascular events. J. Clin. Hypertens. *21*, 421–425. https://doi.org/10.1111/jch.13489.
80. Duvallet, C., Gibbons, S.M., Gurry, T., Irizarry, R.A., and Alm, E.J. (2017). Meta-analysis of gut microbiome studies identifies disease-specific and

shared responses. Nat. Commun. *8*, 1784. https://doi.org/10.1038/s41467-017-01973-8.

81. Feng, Z., Long, W., Hao, B., Ding, D., Ma, X., Zhao, L., and Pang, X. (2017). A human stool-derived Bilophila wadsworthia strain caused systemic inflammation in specific-pathogen-free mice. Gut Pathog. *9*, 59. https://doi.org/10.1186/s13099-017-0208-7.
82. Natividad, J.M., Lamas, B., Pham, H.P., Michel, M.-L., Rainteau, D., Bridonneau, C., da Costa, G., van Hylckama Vlieg, J., Sovran, B., Chamignon, C., et al. (2018). Bilophila wadsworthia aggravates high fat diet induced metabolic dysfunctions in mice. Nat. Commun. *9*, 2802. https://doi.org/10.1038/s41467-018-05249-7.
83. Cani, P.D., Depommier, C., Derrien, M., Everard, A., and de Vos, W.M. (2022). Akkermansia muciniphila: paradigm for next-generation beneficial microorganisms. Nat. Rev. Gastroenterol. Hepatol. *19*, 625–637. https://doi.org/10.1038/s41575-022-00631-9.
84. Minnebo, Y., Delbaere, K., Goethals, V., Raes, J., Van de Wiele, T., and De Paepe, K. (2023). Gut microbiota response to in vitro transit time variation is mediated by microbial growth rates, nutrient use efficiency and adaptation to in vivo transit time. Microbiome *11*, 240. https://doi.org/10.1186/s40168-023-01691-y.
85. Mallick, H., Rahnavard, A., McIver, L.J., Ma, S., Zhang, Y., Nguyen, L.H., Tickle, T.L., Weingart, G., Ren, B., Schwager, E.H., et al. (2021). Multivariable association discovery in population-scale meta-omics studies. PLoS Comput. Biol. *17*, e1009442. https://doi.org/10.1371/journal.pcbi.1009442.
86. Wirbel, J., Essex, M., Forslund, S.K., and Zeller, G. (2022). Evaluation of microbiome association models under realistic and confounded conditions. Preprint at bioRxiv. https://doi.org/10.1101/2022.05.09.491139.
87. Woting, A., Pfeiffer, N., Loh, G., Klaus, S., and Blaut, M. (2014). Clostridium ramosum promotes high-fat diet-induced obesity in gnotobiotic mouse models. mBio *5*, e01530-14. https://doi.org/10.1128/mBio.01530-14.
88. Crost, E.H., Coletto, E., Bell, A., and Juge, N. (2023). Ruminococcus gnavus: friend or foe for human health. FEMS Microbiol. Rev. *47*, fuad014. https://doi.org/10.1093/femsre/fuad014.
89. Mosca, A., Leclerc, M., and Hugot, J.P. (2016). Gut microbiota diversity and human diseases: should we reintroduce key predators in our ecosystem? Front. Microbiol. *7*, 455. https://doi.org/10.3389/fmicb.2016.00455.
90. Kriss, M., Hazleton, K.Z., Nusbacher, N.M., Martin, C.G., and Lozupone, C.A. (2018). Low diversity gut microbiota dysbiosis: drivers, functional implications and recovery. Curr. Opin. Microbiol. *44*, 34–40. https://doi.org/10.1016/j.mib.2018.07.003.
91. Reisinger, E.C., Fritzsche, C., Krause, R., and Krejs, G.J. (2005). Diarrhea caused by primarily non-gastrointestinal infections. Nat. Rev. Gastroenterol. Hepatol. *2*, 216–222. https://doi.org/10.1038/ncpgasthep0167.
92. Navaneethan, U., and Giannella, R.A. (2008). Mechanisms of infectious diarrhea. Nat. Clin. Pract. Gastroenterol. Hepatol. *5*, 637–647. https://doi.org/10.1038/ncpgasthep1264.
93. Binder, H.J. (2009). Mechanisms of diarrhea in inflammatory bowel diseases. Ann. N. Y. Acad. Sci. *1165*, 285–293. https://doi.org/10.1111/j.1749-6632.2009.04039.x.
94. Fu, P., Gao, M., and Yung, K.K.L. (2020). Association of intestinal disorders with Parkinson's disease and Alzheimer's disease: A systematic review and meta-analysis. ACS Chem. Neurosci. *11*, 395–405. https://doi.org/10.1021/acschemneuro.9b00607.
95. Gulick, E.E. (2022). Neurogenic bowel dysfunction over the course of multiple sclerosis: a review. Int. J. MS Care *24*, 209–217. https://doi.org/10.7224/1537-2073.2021-007.
96. Guérin, A., Mody, R., Fok, B., Lasch, K.L., Zhou, Z., Wu, E.Q., Zhou, W., and Talley, N.J. (2014). Risk of developing colorectal cancer and benign colorectal neoplasm in patients with chronic constipation. Aliment. Pharmacol. Ther. *40*, 83–92. https://doi.org/10.1111/apt.12789.
97. Ueki, T., and Nakashima, M. (2019). Relationship between constipation and medication. J. UOEH *41*, 145–151. https://doi.org/10.7888/juoeh.41.145.
98. Pasolli, E., Truong, D.T., Malik, F., Waldron, L., and Segata, N. (2016). Machine learning meta-analysis of large metagenomic datasets: tools and biological insights. PLOS Comput. Biol. *12*, e1004977. https://doi.org/10.1371/journal.pcbi.1004977.
99. Wirbel, J., Zych, K., Essex, M., Karcher, N., Kartal, E., Salazar, G., Bork, P., Sunagawa, S., and Zeller, G. (2021). Microbiome meta-analysis and cross-disease comparison enabled by the SIAMCAT machine learning toolbox. Genome Biol. *22*, 93. https://doi.org/10.1186/s13059-021-02306-1.
100. Miquel, S., Martín, R., Rossi, O., Bermúdez-Humarán, L.G., Chatel, J.M., Sokol, H., Thomas, M., Wells, J.M., and Langella, P. (2013). Faecalibacterium prausnitzii and human intestinal health. Curr. Opin. Microbiol. *16*, 255–261. https://doi.org/10.1016/j.mib.2013.06.003.
101. Li, H., and Durbin, R. (2009). Fast and accurate short read alignment with Burrows-Wheeler transform. Bioinformatics *25*, 1754–1760. https://doi.org/10.1093/bioinformatics/btp324.
102. Huerta-Cepas, J., Forslund, K., Coelho, L.P., Szklarczyk, D., Jensen, L.J., von Mering, C., and Bork, P. (2017). Fast genome-wide functional annotation through orthology assignment by eggNOG-mapper. Mol. Biol. Evol. *34*, 2115–2122. https://doi.org/10.1093/molbev/msx148.
103. Le Meur, N., Hahne, F., Ellis, B., and Haaland, P. (2007). FlowCore: Data Structures Package for Flow Cytometry Data (Bioconductor Project).
104. Wu, T., Hu, E., Xu, S., Chen, M., Guo, P., Dai, Z., Feng, T., Zhou, L., Tang, W., Zhan, L., et al. (2021). clusterProfiler 4.0: A universal enrichment tool for interpreting omics data. Innov. J. *2*, 100141. https://doi.org/10.1016/j.xinn.2021.100141.
105. Oksanen, J. (2007). Multivariate Analysis of Ecological Communities in R: Vegan Tutorial (University of Oulu).
106. Kuhn, M. (2008). Building predictive models in R using the caret package. J. Stat. Softw. *28*, 1–26.
107. Ho, D.E., Imai, K., King, G., and Stuart, E.A. (2011). MatchIt: nonparametric preprocessing for parametric causal inference. J. Stat. Softw. *42*, 1–28. https://doi.org/10.18637/jss.v042.i08.
108. Fan, Y., Støving, R.K., Berreira Ibraim, S., Hyötyläinen, T., Thirion, F., Arora, T., Lyu, L., Stankevic, E., Hansen, T.H., Déchelotte, P., et al. (2023). The gut microbiota contributes to the pathogenesis of anorexia nervosa in humans and mice. Nat. Microbiol. *8*, 787–802. https://doi.org/10.1038/s41564-023-01355-5.
109. Huerta-Cepas, J., Szklarczyk, D., Heller, D., Hernández-Plaza, A., Forslund, S.K., Cook, H., Mende, D.R., Letunic, I., Rattei, T., Jensen, L.J., et al. (2019). eggNOG 5.0: a hierarchical, functionally and phylogenetically annotated orthology resource based on 5090 organisms and 2502 viruses. Nucleic Acids Res. *47*, D309–D314. https://doi.org/10.1093/nar/gky1085.
110. Kanehisa, M., Furumichi, M., Sato, Y., Kawashima, M., and Ishiguro-Watanabe, M. (2023). KEGG for taxonomy-based analysis of pathways and genomes. Nucleic Acids Res. *51*, D587–D592. https://doi.org/10.1093/nar/gkac963.
111. Thiele, M., Detlefsen, S., Sevelsted Møller, L., Madsen, B.S., Fuglsang Hansen, J., Fialla, A.D., Trebicka, J., and Krag, A. (2016). Transient and 2-dimensional Shear-Wave elastography provide comparable assessment of alcoholic liver fibrosis and cirrhosis. Gastroenterology *150*, 123–133. https://doi.org/10.1053/j.gastro.2015.09.040.
112. Thiele, M., Madsen, B.S., Hansen, J.F., Detlefsen, S., Antonsen, S., and Krag, A. (2018). Accuracy of the enhanced liver fibrosis Test vs FibroTest, elastography, and indirect markers in detection of advanced fibrosis in patients with alcoholic liver disease. Gastroenterology *154*, 1369–1379. https://doi.org/10.1053/j.gastro.2018.01.005.
113. Rasmussen, D.N., Thiele, M., Johansen, S., Kjærgaard, M., Lindvig, K.P., Israelsen, M., Antonsen, S., Detlefsen, S., Krag, A., Galaxy, et al. (2021).

Prognostic performance of 7 biomarkers compared to liver biopsy in early alcohol-related liver disease. J. Hepatol. *75*, 1017–1025. https://doi.org/10.1016/j.jhep.2021.05.037.

114. Niu, L., Thiele, M., Geyer, P.E., Rasmussen, D.N., Webel, H.E., Santos, A., Gupta, R., Meier, F., Strauss, M., Kjaergaard, M., et al. (2022). Noninvasive proteomic biomarkers for alcohol-related liver disease. Nat. Med. *28*, 1277–1287. https://doi.org/10.1038/s41591-022-01850-y.

115. Thiele, M., Suvitaival, T., Trošt, K., Kim, M., de Zawadzki, A., Kjaergaard, M., Rasmussen, D.N., Lindvig, K.P., Israelsen, M., Detlefsen, S., et al. (2023). Sphingolipids are depleted in alcohol-related liver fibrosis. Gastroenterology *164*, 1248–1260. https://doi.org/10.1053/j.gastro.2023.02.023.

116. Madsen, B.S., Trebicka, J., Thiele, M., Israelsen, M., Arumugan, M., Havelund, T., and Krag, A. (2018). Antifibrotic and molecular aspects of Rifaximin in alcoholic liver disease: study protocol for a randomized controlled trial. Trials *19*, 143. https://doi.org/10.1186/s13063-018-2523-9.

117. Israelsen, M., Madsen, B.S., Torp, N., Johansen, S., Hansen, C.D., Detlefsen, S., Andersen, P., Hansen, J.K., Lindvig, K.P., Rasmussen, D.N., et al. (2023). Rifaximin-α for liver fibrosis in patients with alcohol-related liver disease (GALA-RIF): a randomised, double-blind, placebo-controlled, phase 2 trial. Lancet Gastroenterol. Hepatol. *8*, 523–532. https://doi.org/10.1016/S2468-1253(23)00010-9.

118. Israelsen, M., Kim, M., Suvitaival, T., Madsen, B.S., Hansen, C.D., Torp, N., Trost, K., Thiele, M., Hansen, T., Legido-Quigley, C., et al. (2021). Comprehensive lipidomics reveals phenotypic differences in hepatic lipid turnover in ALD and NAFLD during alcohol intoxication. JHEP Rep. *3*, 100325. https://doi.org/10.1016/j.jhepr.2021.100325.

119. Torp, N., Israelsen, M., Nielsen, M.J., Åstrand, C.P., Juhl, P., Johansen, S., Hansen, C.D., Madsen, B., Villesen, I.F., Leeming, D.J., et al. (2022). Binge drinking induces an acute burst of markers of hepatic fibrogenesis (PRO-C3). Liver Int. *42*, 92–101. https://doi.org/10.1111/liv.15120.

120. Israelsen, M., Alvarez-Silva, C., Madsen, B.S., Hansen, C.D., Torp, N.C., Johansen, S., Hansen, J.K., Prier Lindvig, K.P., Insonere, J., Riviere, V., et al. (2024). Impact of acute alcohol consumption on circulating microbiome in asymptomatic alcohol-related liver disease. Gut *73*, 1041–1044. https://doi.org/10.1136/gutjnl-2023-330360.

121. Stankevic, E., Israelsen, M., Juel, H.B., Madsen, A.L., Ängquist, L., Aldiss, P.S.J., Torp, N., Johansen, S., Hansen, C.D., Hansen, J.K., et al. (2023). Binge drinking episode causes acute, specific alterations in systemic and hepatic inflammation-related markers. Liver Int. *43*, 2680–2691. https://doi.org/10.1111/liv.15692.

122. Brøns, C., Thuesen, A.C.B., Elingaard-Larsen, L.O., Justesen, L., Jensen, R.T., Henriksen, N.S., Juel, H.B., Størling, J., Ried-Larsen, M., Sparks, L.M., et al. (2022). Increased liver fat associates with severe metabolic perturbations in low birth weight men. Eur. J. Endocrinol. *186*, 511–521. https://doi.org/10.1530/EJE-21-1221.

123. Elingaard-Larsen, L.O., Villumsen, S.O., Justesen, L., Thuesen, A.C.B., Kim, M., Ali, M., Danielsen, E.R., Legido-Quigley, C., van Hall, G., Hansen, T., et al. (2023). Circulating metabolomic and lipidomic signatures identify a type 2 diabetes risk profile in low-birth-weight men with non-alcoholic fatty liver disease. Nutrients *15*, 1590. https://doi.org/10.3390/nu15071590.

124. Holm, J.-C., Gamborg, M., Bille, D.S., Gr Nb K, H.N., Ward, L.C., and Faerk, J. (2011). Chronic care treatment of obese children and adolescents. Int. J. Pediatr. Obes. *6*, 188–196. https://doi.org/10.3109/17477166.2011.575157.

125. Lehmann, J.M., Claus, K., Jansen, C., Pohlmann, A., Schierwagen, R., Meyer, C., Thomas, D., Manekeller, S., Claria, J., Strassburg, C.P., et al. (2018). Circulating CXCL10 in cirrhotic portal hypertension might reflect systemic inflammation and predict ACLF and mortality. Liver Int. *38*, 875–884. https://doi.org/10.1111/liv.13610.

126. Torner, M., Mangal, A., Scharnagl, H., Jansen, C., Praktiknjo, M., Queck, A., Gu, W., Schierwagen, R., Lehmann, J., Uschner, F.E., et al. (2020). Sex specificity of kidney markers to assess prognosis in cirrhotic patients with TIPS. Liver Int. *40*, 186–193. https://doi.org/10.1111/liv.14230.

127. Blaya, D., Pose, E., Coll, M., Lozano, J.J., Graupera, I., Schierwagen, R., Jansen, C., Castro, P., Fernandez, S., Sidorova, J., et al. (2021). Profiling circulating microRNAs in patients with cirrhosis and acute-on-chronic liver failure. JHEP Reports *3*, 100233. https://doi.org/10.1016/j.jhepr.2021.100233.

128. Wirtz, T.H., Reuken, P.A., Jansen, C., Fischer, P., Bergmann, I., Backhaus, C., Emontzpohl, C., Reißing, J., Brandt, E.F., Koenen, M.T., et al. (2021). Balance between macrophage migration inhibitory factor and sCD74 predicts outcome in patients with acute decompensation of cirrhosis. JHEP Rep. *3*, 100221. https://doi.org/10.1016/j.jhepr.2020.100221.

129. Coelho, L.P., Alves, R., Monteiro, P., Huerta-Cepas, J., Freitas, A.T., and Bork, P. (2019). NG-meta-profiler: fast processing of metagenomes using NGLess, a domain-specific language. Microbiome *7*, 84. https://doi.org/10.1186/s40168-019-0684-8.

130. Keller, M.I., Nishijima, S., Podlesny, D., Kim, C.Y., Robbani, S.M., Schudoma, C., Fullam, A., Richter, J., Letunic, I., Akanni, W., et al. (2024). Refined Enterotyping reveals dysbiosis in global fecal metagenomes. Preprint at bioRxiv. https://doi.org/10.1101/2024.08.13.607711.

131. Schmidt, T.S.B., Fullam, A., Ferretti, P., Orakov, A., Maistrenko, O.M., Ruscheweyh, H.-J., Letunic, I., Duan, Y., Van Rossum, T., Sunagawa, S., et al. (2024). SPIRE: a searchable, planetary-scale mIcrobiome REsource. Nucleic Acids Res. *52*, D777–D783. https://doi.org/10.1093/nar/gkad943.

132. Weingarden, A., González, A., Vázquez-Baeza, Y., Weiss, S., Humphry, G., Berg-Lyons, D., Knights, D., Unno, T., Bobr, A., Kang, J., et al. (2015). Dynamic changes in short- and long-term bacterial composition following fecal microbiota transplantation for recurrent Clostridium difficile infection. Microbiome *3*, 10. https://doi.org/10.1186/s40168-015-0070-0.

133. Yatsunenko, T., Rey, F.E., Manary, M.J., Trehan, I., Dominguez-Bello, M.G., Contreras, M., Magris, M., Hidalgo, G., Baldassano, R.N., Anokhin, A.P., et al. (2012). Human gut microbiome viewed across age and geography. Nature *486*, 222–227. https://doi.org/10.1038/nature11053.

134. Nishijima, S., Nagata, N., Kiguchi, Y., Kojima, Y., Miyoshi-Akiyama, T., Kimura, M., Ohsugi, M., Ueki, K., Oka, S., Mizokami, M., et al. (2022). Extensive gut virome variation and its associations with host and environmental factors in a population-level cohort. Nat. Commun. *13*, 5252. https://doi.org/10.1038/s41467-022-32832-w.

135. Leitsalu, L., Haller, T., Esko, T., Tammesoo, M.-L., Alavere, H., Snieder, H., Perola, M., Ng, P.C., Mägi, R., Milani, L., et al. (2015). Cohort profile: Estonian biobank of the Estonian Genome Center, University of Tartu. Int. J. Epidemiol. *44*, 1137–1147. https://doi.org/10.1093/ije/dyt268.

136. Benjamini, Y., and Hochberg, Y. (1995). Controlling the false discovery rate: A practical and powerful approach to multiple testing. J. R. Stat. Soc. B *57*, 289–300. https://doi.org/10.1111/j.2517-6161.1995.tb02031.x.

137. Nagata, N., Nishijima, S., Kojima, Y., Hisada, Y., Imbe, K., Miyoshi-Akiyama, T., Suda, W., Kimura, M., Aoki, R., Sekine, K., et al. (2022). Metagenomic identification of microbial signatures predicting pancreatic cancer from a multinational study. Gastroenterology *163*, 222–238. https://doi.org/10.1053/j.gastro.2022.03.054.

138. Louis, S., Tappu, R.M., Damms-Machado, A., Huson, D.H., and Bischoff, S.C. (2016). Characterization of the Gut Microbial Community of Obese Patients Following a Weight-Loss Intervention Using Whole Metagenome Shotgun Sequencing. PLoS One *11*, e0149564. https://doi.org/10.1371/journal.pone.0149564.

STAR★METHODS

KEY RESOURCES TABLE

REAGENT or RESOURCE	SOURCE	IDENTIFIER
Chemicals, peptides, and recombinant proteins		
2% Paraformaldehyde	VWR	J61899.AP
SYBR Green I	Fisher Scientific	S7563
Dimethylsulfoxide	Sigma-Aldrich	D8418-100ML
123count eBeads	Invitrogen	01-1234-42
Critical commercial assays		
AllPrep PowerFecal Pro DNA/RNA Kit	Qiagen	80254
NEBNext Ultra II DNA Library Prep kit	New England Biolabs	E7645L
Deposited data		
Shotgun metagenomic data (GALA-ALD)	This study	BioProject: PRJEB76661
Shotgun metagenomic data (GALA-HP)	This study	BioProject: PRJEB76664
Shotgun metagenomic data (GALA-RIF)	This study	BioProject: PRJEB76667
Shotgun metagenomic data (AlcoChallenge)	This study	BioProject: PRJEB76662
Shotgun metagenomic data (HCO)	This study	BioProject: PRJEB81698
Shotgun metagenomic data (GALA-POSTBIO)	This study	BioProject: PRJEB76668
Shotgun metagenomic data (GastricBypass)	This study	BioProject: PRJEB76666
Shotgun metagenomic data (HOLBAEK)	This study	BioProject: PRJEB81697
Shotgun metagenomic data (TIPS)	This study	BioProject: PRJEB76665
Software and algorithms		
mOTUs (v2.5)	Milanese et al.[37]	https://motu-tool.org/
BWA-MEM (v0.7.17)	Li and Durbin[101]	https://github.com/lh3/bwa
eggNOG-mapper (v1.0.3)	Huerta-Cepas et al.[102]	https://github.com/eggnogdb/eggnog-mapper
flowcore R package (v1.11.20)	Le Meur et al.[103]	https://bioconductor.org/packages/release/bioc/html/flowCore.html
clusterProfiler R package (v4.8.3)	Wu et al.[104]	https://www.bioconductor.org/packages/release/bioc/html/clusterProfiler.html
vegan R package (v2.6.4)	Oksanen[105]	https://cran.r-project.org/web/packages/vegan/index.html
xgboost R package (v1.7.5.1)	Chen and Guestrin[47]	https://cran.r-project.org/web/packages/xgboost/index.html
caret R package (v6.0.94)	Kuhn[106]	https://cran.r-project.org/web/packages/caret/index.html
MatchIt R package (v4.5.3)	Ho et al.[107]	https://kosukeimai.github.io/MatchIt/
BD FACSDiVa software	Becton, Dickinson and Company	https://www.bdbiosciences.com/en-dk/products/software/instrument-software/bd-facsdiva-software
Flowcore R package (v1.11.20)	Meur et al.[108]	https://bioconductor.org/packages/flowCore/
Other		
Shotgun metagenomic data (MetaCardis)	Vieira-Silva et al.,[33] Forslund et al.,[34] and Fromentin et al.[35]	PRJEB41311, PRJEB38742, and PRJEB37249
Microbial load data (MetaCardis)	Forslund et al.[34]	N/A
Shotgun metagenomic data (Estonian Microbiome)	Aasmets et al.[58]	EGAS00001008448

(*Continued on next page*)

Continued

REAGENT or RESOURCE	SOURCE	IDENTIFIER
Shotgun metagenomic data (Japanese 4D)	Nagata et al.[57]	N/A
GMGC	Coelho et al.[38]	https://gmgc.embl.de/
eggNOG	Huerta-Cepas et al.[109]	http://eggnog5.embl.de/
KEGG	Kanehisa M. et al.[110]	https://www.genome.jp/kegg/

EXPERIMENTAL MODEL AND STUDY PARTICIPANT DETAILS

GALAXY/MicrobLiver study population

A total of 1,906 fecal samples were collected in the GALAXY/MicrobLiver study population. These samples were derived from 9 different cohorts (GALA-ALD,[111–113] GALA-HP,[114,115] GALA-RIF,[116,117] AlcoChallenge,[118–121] High Carbohydrate Overfeeding (HCO),[122,123] GALA-POSTBIO, GastricBypass, The HOLBAEK Study (HOLBAEK),[124] and TIPS[125–128]) with different study designs and objectives. These studies involved diverse participant groups, including healthy individuals (GALA-HP), patients with chronic alcohol-related liver disease (ALD) (GALA-ALD and TIPS), those with severe obesity (GastricBypass), those born with low birth weight (HCO), children and adolescents with obesity (HOLBAEK), and patients with dietary (GALA-POSTBIO), alcohol (AlcoChallenge), and drug interventions (GALA-RIF). Out of the 1,906 samples, 12 samples were excluded as outliers from the downstream analyses due to having substantially lower microbial loads than other samples (<10% of the median value of the samples). In total, 1,894 fecal samples from 1,351 participants were used in the study (Table S1A). The objective of each cohort, study design, inclusion, and exclusion criteria were described as follows.

GALA-ALD

This is a prospective, single-center, biopsy-controlled, cross-sectional study covering the full range of alcohol-related liver disease (ALD).[111–113] Patients were recruited between 2013 and 2018 in the Region of Southern Denmark. Inclusion criteria comprised individuals aged 18-75 years with prior or current chronic alcohol overuse, which was defined as more than 24 g/day for women and more than 36 g/day for men for over a year, and informed consent to a liver biopsy. Exclusion criteria included solid evidence of cirrhosis, concurrent liver diseases, severe illnesses with less than 12 months expected survival, contraindications to percutaneous liver biopsy, severe alcohol-related hepatitis, hepatic congestion or bile duct dilation as shown by ultrasound, HIV positive status, ongoing substance abuse other than alcohol, and inability to comply with the study protocol. Participants were sourced from both primary and secondary healthcare, encompassing populations at low versus moderate-high prevalence of cirrhosis.

GALA-HP

This longitudinal study involved healthy participants recruited between 2016 and 2018 at Odense University Hospital in Denmark. The inclusion criteria specified individuals aged 18-75 who were matched by sex, age and (partially) BMI to patients from the GALA-ALD study.[114,115] The exclusion criteria included current alcohol consumption exceeding 7 units per week, prior harmful alcohol use, known liver disease, elevated liver enzymes or altered liver function tests, signs of altered glucose metabolism, signs of other metabolic diseases, infection/inflammation, significant vitamin/mineral deficiencies, any known chronic diseases, ongoing substance abuse, use of any medication (besides infrequent use of mild pain relievers), and use of antibiotics within the last six months. Stool samples were collected at home, frozen in the home freezer immediately, and brought to our unit (with cooling elements to remain frozen) for –80 °C storage within 24 hours.

The study protocol for the GALA-ALD and GALA-HP was approved by the ethics committee for the Region of Southern Denmark (nos. S-20160006G, S-20120071, S-20160021 and S-20170087) and is registered with both the Danish Data Protection Agency (nos. 13/8204, 16/3492 and 18/22692) and Odense Patient Data Exploratory Network (under study identification nos. OP_040 and OP_239 [open.rsyd.dk/OpenProjects/da/openProjectList.jsp]). These studies were conducted according to the principles of the Declaration of Helsinki, and oral and written informed consent was obtained from all participants.

GALA-RIF

The GALA-RIF trial, an investigator-initiated, randomized, double-blind, placebo-controlled, single-center, phase 2 study, was conducted to evaluate the efficacy of rifaximin-α in patients diagnosed with alcohol-related liver disease through liver biopsy.[116,117] Patients were allocated in a 1:1 ratio to either rifaximin-α or placebo for 18 months. Patients were recruited at the Department of Gastroenterology and Hepatology at Odense University Hospital in Denmark. Ethical approval was granted by the regional ethics committee (S-20140078), and the study adhered to the International Conference on Harmonization Good Clinical Practice guidelines, with external monitoring by the Good Clinical Practice Unit at Odense University Hospital. Participants were identified from a cross-sectional study (GALA-ALD) focusing on alcohol-related liver disease. Alcohol overuse was defined as a daily intake of 24g or more for women and 36g or more for men for at least a year. The study excluded patients with a history of hepatic decompensation

or any known liver disease. Following the screening, patients at risk of liver fibrosis underwent liver biopsy. From these, patients aged 18–75 years with liver fibrosis and histological features of alcohol-related liver disease were included in the study. Stool samples analyzed in this study were derived from baseline, 1 month, and 18 months (at the end of treatment). EudraCT, number: 2014–001856-51.

AlcoChallenge

This clinical study aimed to investigate the acute impact of alcohol consumption on the intestine with the hypothesis that acute alcohol intake increased intestinal permeability and inflow of bacterial products to the liver.[118–121] Participants aged 18-75 who met the criteria for ALD, metabolic dysfunction-associated steatotic liver disease (MASLD), or healthy controls were included. Patients with other known causes of liver disease, total alcohol abstinence or desire for it, insulin-dependent diabetes mellitus, cirrhosis, pregnancy, recent antibiotic treatment, liver cancer, severe comorbidities, or inability to follow instructions were excluded. Participants were asked to maintain their habitual diet and alcohol consumption until two days before the alcohol intervention. On the investigation day, participants were fasting and abstained from alcohol for 48 hours. Stool samples were collected by the participants within 24 hours of each visit. Participants were given instructions and material for sample collection. The samples were collected in sealed test tubes and stored immediately in the participants' freezer. The samples were transported to the hospital as cold as possible using a cooler bag and cooling elements. Upon arrival at the hospital, the samples were stored in a –80 °C freezer. The study was approved by the Ethical Committee of Southern Denmark (S-20160083) and registered at ClinicalTrials.gov (NCT03018990).

HCO

This study aims to investigate whether 12 weeks of exercise training can revert and/or minimize the deleterious cardiometabolic effects of 4 weeks of carbohydrate overfeeding in individuals born with low birth weight and increased risk of developing type 2 diabetes. This study recruited healthy Caucasian males, born between 1979 and 1980 at full term (gestational weeks 39–41).[122,123] Exclusion criteria for participants included having diabetes in their first-degree relatives, any chronic or acute diseases, medication intake that could affect the study's outcomes, BMI > 30 kg/m^2, physical activity >10 hours per week, alcohol consumption exceeding the national recommendations, and significant weight changes (>2 kg) in the past 6 months. Feces were sampled at home and immediately stored in the freezer at –18 °C or cooler. The samples were picked up by the staff and transported on dry ice to the laboratory and stored at –80 °C. The study was conducted in compliance with the Declaration of Helsinki II and approved by the ethical committee of the Capital Region of Denmark, with identifier H-4-2014-128. The research has been registered under the ClinicalTrials.gov identifier: NCT02982408. All participants provided written informed consent to participate in the study.

GALA-POSTBIO

A 24-week prospective, randomized controlled clinical trial aiming to investigate if a postbiotic drink made of fermented oats, ReFerm®, could alter the progression of liver disease compared to an active comparator, Fresubin®. From March 2019 to January 2021, 56 patients were recruited and included in the study. The trial was held at the Department of Gastroenterology and Hepatology at Odense University Hospital in Denmark. Ethical approval was granted by the regional ethics committee (S-20170163) and the Danish Data Protection Agency (19/6646). Patients were allocated in a 1:1 ratio to either ReFerm® or Fresubin® treatment groups. Clinical investigations were conducted at baseline, 4 weeks, 24 weeks (end of intervention), and after a wash-out period of 6 to 8 weeks. Inclusion criteria were outpatients with stable, compensated advanced chronic alcohol-related liver disease between 30 and 75 years. Compensated advanced chronic alcohol-related liver disease was defined as liver stiffness ≥15 kPa or a newly performed (<6mdr) liver biopsy with Kleiner Fibrosis Stage ≥ 3 or a liver biopsy > 6 months with Kleiner Fibrosis Stage ≥ 3 and a current liver stiffness ≥10 kPa. Eligible patients had a prior or ongoing harmful alcohol intake defined as an average of ≥24g alcohol/day for women and ≥36 g/d for men for ≥ 5 years. Exclusion criteria were Child-Pugh C score, Meld-Na ≥15, hospitalization within three months, moderate or severe ascites, high-risk varices needing interventional treatment, known liver disease other than alcohol-related, antibiotic treatment in the prior three months, and treatment with nutritional drinks, probiotics or prebiotics within the last three months. ClinicalTrials.gov ID: NCT03863730.

GastricBypass

The bariatric study cohort is based on 70 patients with a BMI > 35.0 kg/m2 undergoing laparoscopic bariatric surgery (either Roux-en-Y gastric bypass (*n*=30) or sleeve gastrectomy (*n*=40)). The design is best described as a prospective cohort study. Study subjects were included between December 2016 and September 2019 at Copenhagen University Hospital Hvidovre. The study subjects fulfilled the existing criteria for bariatric surgery issued by the Danish Health Authorities (BMI>35.0 kg and metabolic comorbidity and/or arthrosis in lower extremities OR BMI>50 with or without metabolic comorbidity/arthrosis in lower extremities), including a mandatory weight loss of 8% before surgery. The mode of surgery (Roux-en-Y gastric bypass or sleeve gastrectomy) was decided by the endocrinologists at the Endocrinology Department. Study-specific exclusion criteria were current or previous alcohol consumption of > 2.5 units/day for men and > 1.5 units/day for women, use of antibiotics within one month prior to surgery, preexisting liver disease other than metabolic dysfunction-associated steatotic liver disease, pre-existing disease in the lipid metabolism and acute or chronic inflammatory disease, or an ethnic origin other than North European. On the day of surgery (aka baseline visit) fasting project blood samples were collected. The fecal samples were collected 1-7 days prior to surgery and immediately frozen. During surgery, liver and

adipose tissue were sampled. Follow-up visits including collection of fecal- and blood samples were conducted three, six, and 12 months after surgery. Fecal samples at the baseline, three, and 12 months were analyzed in this study. The study protocol was approved by the Regional Scientific Ethics Committee (H-16030784 and H-16030782). Written and oral informed consent was obtained from all study participants. The study was conducted according to the Declaration of Helsinki.

The HOLBAEK Study

We collected fecal samples from 397 5–19-year-olds of which 331 were from a hospital-based obesity clinic cohort and 66 were from a population-based cohort. The hospital-based obesity clinic cohort consists of children and adolescents enrolled in multifaceted obesity management from January 2008 onwards at the Children's Obesity Clinic, Holbaek University Hospital.[124] These patients were referred from general practitioners, pediatric departments, or community-based doctors. In the hospital-based obesity clinic cohort, the longitudinal data collection began just prior to the initiation of non-pharmacological obesity treatment and continued with the subsequent contacts in the clinic in a systematic, family-based, person-centred, chronic care setting. The only inclusion criterion was a referral to the hospital-based obesity clinic. Importantly, no a priori age- or other exclusion criteria would make a child or adolescent ineligible for treatment or inclusion in the clinic. The population-based cohort consists of children and adolescents recruited from October 2010 onwards without selection pertaining to body weight or BMI. Recruitment took place at schools and high schools across 11 municipalities in Region Zealand and the Capital Region in Denmark. All children and adolescents at the participating schools were considered eligible for inclusion regardless of age, and no exclusion criteria were applied. Informative recruitment meetings for potential participants were held during school hours and written material was delivered to the parents. Stool samples were collected at participants' homes, immediately frozen in their home freezers, and then transported to the laboratory with cooling elements to ensure they remained frozen. Upon arrival, the samples were stored in freezers at a temperature of –80 °C within 24 hours of collection. The HOLBAEK Study was approved by the Ethical Committee of Region Zealand (Project number: SJ-104), The Danish Data Protection Agency (REG-043-2013), and other collateral project approvals and was registered at ClinicalTrials.gov on June 26, 2009 (NCT00928473). All procedures in relation to the biobank are performed in accordance with the Helsinki Declaration. Written informed consent was obtained from parents/legal guardians or from the adolescents themselves when above the age of 18 years.

TIPS

The TIPS study is a single-center prospective study in patients with decompensated cirrhosis who received a transjugular portosystemic shunt as part of the NEPTUN study (NCT03628807) at the Department of Internal Medicine I, University Clinic Bonn (Germany).[125–128] For this study, stool samples from 84 patients were obtained between 2014 and 2018. The mean age was 58 years (range 18–84 years), 53% of the patients were male and the majority of patients had alcohol-induced cirrhosis (n=62), followed by viral hepatitis (n=8) and other etiologies (n=18). The stool samples were collected during the inpatient treatment of the patients shortly before the TIPS procedure and stored directly at -80 °C degrees until further use. The study was approved by the local ethics committee of the University of Bonn (029/13), and all patients signed an informed written consent in accordance with the Helsinki Declaration.

METHOD DETAILS

DNA sequencing of fecal samples

Microbial DNA was extracted from collected stool samples using Qiagen AllPrep PowerFecal Pro DNA/RNA Kit (Qiagen, Hilden, Germany) following the manufacturer's protocol in the GALA-RIF, AlcoChallenge, HCO, GALA-POSTBIO, and TIPS cohorts. The same protocol, except for an additional phenol-chloroform extraction step after the step of lysing microbial cells, was used in the GALA-ALD, GALA-HP, HOLBAEK, and GastricBypass cohorts. Metagenomic sequencing libraries were prepared using the NEBNext Ultra II DNA Library Prep kit (New England Biolabs, MA, USA) with a targeted insert size of 350-400bp and Dual Index multiplex oligos. Libraries were prepared using a liquid automated system (Beckman Coulter i7 Series) and sequenced on an Illumina HiSeq 4000 platform (Illumina, San Diego, CA, USA) with 2x150bp paired-end reads.

Quality control of sequenced reads

Sequenced reads were processed to remove low-quality reads and host-derived reads using ngless (v1.1).[129] Nucleotide calls with a Phred quality score of less than 25 were removed from the 3′ end and reads less than 45 nucleotides long after the removal were discarded. Reads representing human DNA were identified by comparing all reads' sequence similarity to the human reference genome (hg38). Any reads with greater than 90% similarity to the human genome were discarded. After this quality control, reads were re-classified as paired or as singles, where, respectively, both or only the forward and reverse reads are present in the final dataset.

Cell counting

Bacterial cell counting was performed as previously described.[108] Briefly, frozen (-80°C) fecal samples were diluted, mechanically homogenized and afterward fixed with 2% Paraformaldehyde (10 min, RT; VWR). To minimize clumps, the samples were filtered

through a cell strainer. The resulting bacterial cell suspension was stained with SYBR Green I (1:200,000 (Fisher Scientific), in DMSO (Sigma-Aldrich)) and incubated in the dark for 30 min. Measurements were performed at a pre-set flow rate of 0.5 μL/sec, and a known concentration of 123count eBeads (Invitrogen) was added for accurate bacterial cell count estimation. Measurements were performed using a BD Fortessa LSRII flow cytometer (BD Biosciences) (GALA-HP, Alcochallenge, GALA-ALD, TIPS, HCO cohorts) and BD Fortessa 3 flow cytometer (BD Biosciences) (GALA-POSTBIO, GALA-RIF, HOLBAEK, GastricBypass cohorts), and data were acquired using BD FACSDiVa software. A collection threshold value of 200 was applied on the FITC (530/30 nm) channel. Fluorescence intensity was collected at green (530/30 nm, FITC), blue (450/50 nm, Pacific Blue), yellow (575/26 nm, PE), and red (695/40 nm, PerCP-Cy5.5) fluorescence channels. Forward- and side-scattered (FSC and SSC) light intensities were also collected. Data was processed in R using the flowcore package (v1.11.20)[103] in R Studio (v4.1.2). A stringent fixed gating strategy was selected based on density plots of blank sample, unstained fecal sample solution, and stained fecal sample solution. To allow for direct comparison between measured samples, the same gating strategy was applied to all samples. The gating on density plots of the green (FITC-H) channel versus the forward-scatter (FSC-H) channel allowed for a distinction between the stained bacterial cells and unstained debris. The gating on the blue (Pacific Blue-H) channel versus the green (FITC-H) channel allowed for a distinction between the counting beads and other particles in the sample solution, including bacteria and unstained debris. Bacterial cell counts, estimated from pre-set flow rate, were adjusted with internal control counts, included on each plate, to correct for batch effects.

Taxonomic and functional profiling of metagenomes

Species-level taxonomic profiles of the samples were obtained with the marker-gene-bases method using mOTUs (v2.5).[37] Functional profiles were obtained by mapping metagenomic reads to the sub-catalog of the human gut microbiome in the global microbial gene catalog (GMGC)[38] using BWA-MEM (v0.7.17)[101] with the default parameters. The genes were functionally annotated using eggNOG-mapper (v1.0.3)[102] against eggNOG database 5.0[109] and KEGG orthologies[110] were assigned to each gene. The number of reads mapped to each KEGG orthology was counted using gffquant (v2.9.1) (https://github.com/cschu/gff_quantifier) where the count of the number of reads aligning multiple genes was distributed to each gene by dividing by the number of the genes.

MetaCardis dataset

Fecal metagenomes from the MetaCardis project (n = 1,820)[33–35] were downloaded from the European Nucleotide Archive under the accession numbers PRJEB41311, PRJEB38742 and PRJEB37249. Microbial load data for these samples were obtained in the study of Forslund et al.[34] Out of 1820 samples, eight samples were excluded from the downstream analyses as outliers due to significantly lower or higher microbial loads than other samples (9.7e09 and 1.1e11, respectively). In total, 1,812 samples were used in the following analyses. Taxonomic and functional profiles of the microbiomes were obtained with the same procedure described above.

QUANTIFICATION AND STATISTICAL ANALYSIS

Association analysis between the gut microbiome and microbial loads

To investigate correlations between the microbiome profile (i.e. species-level taxonomic and functional compositions) and the experimentally measured microbial load, Pearson correlation coefficients were calculated between the $\log_{10}$ transformed relative abundance of each microbial species/functions and the microbial load in each cohort separately. Additionally, the analysis was also performed for diversity indexes of the taxonomic profiles such as Shannon diversity, species richness (i.e. the number of detected species), and Simpson diversity. The over-representation of KEGG pathways in the positively- and negatively-correlated functions was identified with the gene set enrichment analysis using the GSEA function in the clusterProfiler package (v4.8.3).[104] Multidimensional Scaling (MDS) analysis was performed using the metaMDS function in the vegan package (v2.6.4),[105] based on a Euclidean distance matrix derived from $\log_{10}$-transformed relative abundance data with half of the minimum non-zero value as pseudocounts. Enterotypes (i.e. *Bacteroides*, *Prevotella*, and Firmicutes types)[39,40] of the gut microbiome were determined using the enterotyper (https://enterotype.embl.de/)[130] using the pam3 model and they were plotted into the MDS ordination using the envfit functions in the vegan package.

Construction of prediction models

To construct machine-learning models to predict the microbial load, we employed the eXtreme Gradient Boosting (XGBoost) algorithm,[47] available in the xgboost R package (v1.7.5.1). Prior to model training, we performed unsupervised feature filtering on the species-level taxonomic profiles of the microbiome to exclude minor species (those with < 0.1% average abundance or < 10% prevalence). The relative abundances of each species and the microbial loads were then $\log_{10}$ transformed before the training. For the species, we added half of the non-zero minimum values in the dataset to each abundance to avoid $\log_{10}$ transformation of 0 values, and further standardized (i.e. z-score). The models were trained using the train function in the caret R package (v6.0.94)[106] in the GALAXY/MicrobLiver and MetaCardis datasets separately, employing a 5-times repeated 10-fold cross-validation procedure to maximize the root-mean-square error (RMSE) in the model. The hyperparameters were determined through a grid search. For internal validation, we calculated the average predicted microbial loads across five repetitions for each sample and compared these with the actual microbial loads. For external validation, we applied the GALAXY/MicrobLiver model to the MetaCardis dataset, and vice versa, comparing the predicted and actual microbial loads.

Analysis of 16S rRNA gene data from previous studies

Additional paired data of 16S rRNA gene sequencing and fecal microbial loads were collected from two previous studies.[19,24] For Vandeputte et al.[24] study, the genus-level taxonomic profiles were obtained from the paper. For Vandeputte et al.[19] study, 16S rRNA gene sequencing data were downloaded from the European nucleotide Archive, under the accession numbers PRJEB21504 and ERP023761. The 16S rRNA gene sequencing data was processed using the DADA2 pipeline and the taxonomic annotation was performed using the RDP training data rdp_train_set_16. A prediction model was constructed based on the data of Vandeputte et al.[24] (n = 707) using the same procedure described above. Then, the model was applied to the other dataset of Vandeputte et al.[19] (n = 95) for external validation.

Collection of external microbiome datasets

Global dataset: Publicly available human gut metagenomes were downloaded from the European Nucleotide Archive. The dataset was part of a previous study[131] and was composed of 27,832 samples across 45 countries from 159 studies (Tables S3A and S3B). After the downloading, quality filtering was performed using ngless, and bases with <25 Phred quality score were trimmed from the 3′ end, and reads less than 45 bp were excluded. Host metadata such as age, sex, country, antibiotic treatment, and disease were collected from respective study papers manually. Samples from infants, children under 3 years old, and patients who received fecal microbiota transplantation were excluded since their gut microbiomes are substantially different from those of adults.[132,133] Also, samples with a low number of sequenced reads (ie. <1 million) were excluded. Countries were classified into four groups according to the World Bank definition (https://www.worldbank.org/en/home/, accessed in February 2024), which defines high-income, upper-middle, lower-middle, and low-income economies based on gross national income per capita.

Japanese 4D dataset: The Japanese 4D (Disease, Drug, Diet, Daily life) microbiome cohort is a prospective, multicenter, hospital-based cohort established in the Tokyo metropolitan area. A total of 4,198 fecal samples were collected from the participants and processed as described previously.[57,134] Various intrinsic and extrinsic factors (n = 244) were collected from the participants through a combination of self-reported questionnaires, face-to-face interviews, and physicians' electronic medical records. These factors included anthropometric measurements, lifestyles, dietary habits, physical activities, diseases, and medications (Table S3C). The protocol for the project was approved by the medical ethics committees of the Tokyo Medical University (approval No.: T2019-0119), National Center for Global Health and Medicine (approval No.: 1690), the University of Tokyo (approval No: 2019185NI), Waseda University (approval No.: 2018-318), and the RIKEN Center for Integrative Medical Sciences (approval No.: H30-7). All participants provided written informed consent before participation in the project.

Estonian Microbiome dataset: The Estonian Microbiome cohort[135] is a volunteer-based cohort that currently includes genotyped adults (≥ 18 years old) across Estonia. Fecal samples were collected from 2,509 participants in the cohort and sequenced as described previously.[58] All the participants provided informed consent for the data and samples to be used for scientific purposes. This study received approval from the Research Ethics Committee of the University of Tartu (approval No. 266/T10) and from the Estonian Committee on Bioethics and Human Research (Estonian Ministry of Social Affairs; approval No. 1.1-12/17). Host factors such as anthropometric measurements, lifestyle, diet, disease, and medication were collected from self-reported questionnaires and electronic health records (n = 251, Table S3D).

Evaluation of the effects of biological and technological factors on predicted microbial loads

To assess the impact of technical and biological factors on predicted microbial load, we collected metagenomes from the same fecal samples sequenced in different laboratories (i.e. technical replicates) (n = 40),[48] metagenomes from the same fecal samples sequenced using different DNA extraction methods (n = 185),[49] longitudinal metagenomes obtained from the same individuals (n = 1,294),[50–56] and metagenomes obtained from different individuals (n = 2,369). mOTUs and the MetaCardis model were employed to obtain the species-level taxonomic profile and predicted microbial load, respectively. For longitudinal samples, only pairs with an interval of at least one week were selected, and for individuals with >2 samples, only the first and last pair were included in the analysis. Predicted microbial loads were compared between pairs of technical replicates, between pairs of the same fecal samples with different DNA extraction methods, between pairs of longitudinal samples of the same individuals, and between different individuals. The variation of predicted microbial load in each group was assessed using the coefficient of variation.

Analysis of the external metagenomic datasets

Species-level taxonomic profiles of the global, Japanese 4D, and Estonian Microbiome samples were obtained with the same method described above. The relative abundance of each microbial species was $\log_{10}$-transformed (1e-4 was added as a pseudo count beforehand) and standardized before the prediction. The MetaCardis prediction model was applied to the profiles and microbial loads were predicted for each sample. The MetaCardis model was employed for the analysis since it was trained on samples derived from more individuals (n = 1,812) than the GALAXY/MicrobLiver model (n = 1,351).

To determine the explained variance of the predicted microbial loads (coefficient of determination) by the collected host factors in the Japanese 4D and Estonian Microbiome cohorts, linear regression analysis was performed using the glm function with the $\log_{10}$ transformed microbial load as a response variable and all the host factors as explanatory variables. Furthermore, the analysis was performed for each metadata category (e.g. lifestyle, diet, medication, and disease) separately, and the explained variance by each category was determined. P-values were adjusted for the multiple comparisons with the Benjamini-Hochberg method.[136]

Association analysis between diseases and the microbial load

To explore associations between diseases and microbial loads, we performed a meta-analysis of case-control comparisons by combining samples in the global and Japanese 4D datasets. In the global dataset, 58 studies including at least 10 cases and 10 controls were picked up and the case and control samples were collected (Table S4A). In the Japanese 4D dataset, 9 diseases with >10 patients were selected and age, sex, and BMI matched-controls were defined for each disease using the matchit function of the MatchIt R package (v4.5.3).[107] Disease-to-control ratios were set to 1:4 when there were enough control samples in the Japanese 4D dataset,[137] while set to 1:1 when the number of samples was insufficient.

The case and control samples collected above were combined for each disease and a total of 26 diseases with >50 cases and >50 controls were analyzed (Table S4A). Associations between the diseases and the $\log_{10}$ transformed microbial load were assessed using the glm function with the microbial load as a response variable and the disease condition (i.e. case or control) as an explanatory variable including each study as a covariate. P-values were adjusted for the multiple comparisons with the Benjamini-Hochberg method.

Association analysis between diseases and the microbiome composition

For the 26 diseases selected, case-control comparisons of the microbiome profiles were conducted. For each disease dataset, species with an average relative abundance of >0.1% and prevalence of >10% were included in the analysis. The relative abundance was $\log_{10}$ transformed after adding half of the non-zero minimum value as a pseudo value. For each microbial species, a linear regression model was applied using the glm function. In this model, the species abundance was included as a response variable and disease condition (i.e. case or control) as an explanatory variable, with each study as a covariate. P-values were adjusted for the number of species for each disease with the Benjamini-Hochberg method.[136]

The set of the obtained effect sizes (beta coefficients) of each species was defined as the microbial signature for the disease. A distance matrix among the 26 diseases was then constructed based on the signature, using Spearman's correlation coefficient as a distance metric ([1 - Spearman's correlation] / 2). Then, principal coordinate analysis was performed on this distance matrix using the cmdscale function in the vegan package.[105] The differences in the microbial signatures between the positively- and negatively-associated diseases were examined with permutational analysis of variance using the adonis function in the vegan package with 9,999 permutations for p-value calculation. Additionally, the effect sizes of each disease were compared between the positively- and negatively-associated diseases through a linear regression model, and species discriminating between these two groups were investigated.

To adjust the effect of the microbial load in the case-control comparisons, linear regression models were constructed for each species again by adding the microbial load as a covariate. Effect sizes of each disease on the species and associated *P*-values were compared between the models with and without the adjustment of the microbial load.

Comparison of adjustment based on experimentally measured and predicted microbial loads

To evaluate the robustness of the adjustment for predicted microbial load, we analyzed metagenomes from liver cirrhosis patients in the GALAXY/MicrobLiver study (n = 64, fibrosis stage >F2, GALA-ALD cohort) and type 2 diabetes patients in the MetaCardis study population (n = 539), where both experimentally measured and predicted microbial loads were available. Metagenomes from healthy individuals in the GALAXY/MicrobLiver (n = 127, GALA-HP) and MetaCardis (n = 275) study populations were used as controls. Predicted fecal microbial loads of each sample were obtained by applying the GALAXY/MicrobLiver and MetaCardis models to each other's datasets. The association between each species ($\log_{10}$-transformed relative abundance) and disease was assessed by regression analysis with the glm function, using three methods: no adjustment, with adjustment for actual microbial load, and with adjustment for predicted microbial load. Species with >0.1% average relative abundance and >10% prevalence were included in the analysis in each disease dataset. P-values of each species were corrected for multiple comparisons using the Benjamini-Hochberg method and the differences in the FDR values without adjustment and with adjustment were compared between the methods based on the actual and predicted microbial load.

Comparison of quantitative and relative microbiome profiles in disease association analysis

To explore the advantages of the quantitative microbiome analysis in disease association analysis, we transformed the relative microbiome profiles (RMP) into quantitative microbiome profiles (QMP) (i.e. a profile where species abundances were represented by absolute abundances) by multiplying the relative abundance of each microbial species by the predicted microbial load of the sample. To evaluate the association between each species and disease, the same statistical analyses used for the RMP were performed on the QMP of the same 26 disease datasets. The effect sizes and statistical significance (i.e. *p*-value) obtained from the analyses were compared with those obtained based on the RMP.

CellPress
OPEN ACCESS

Supplemental figures

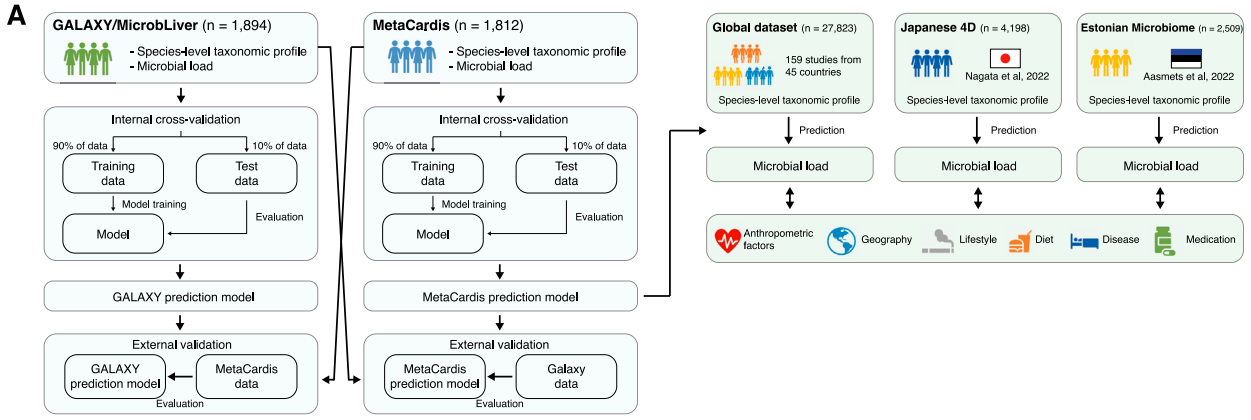

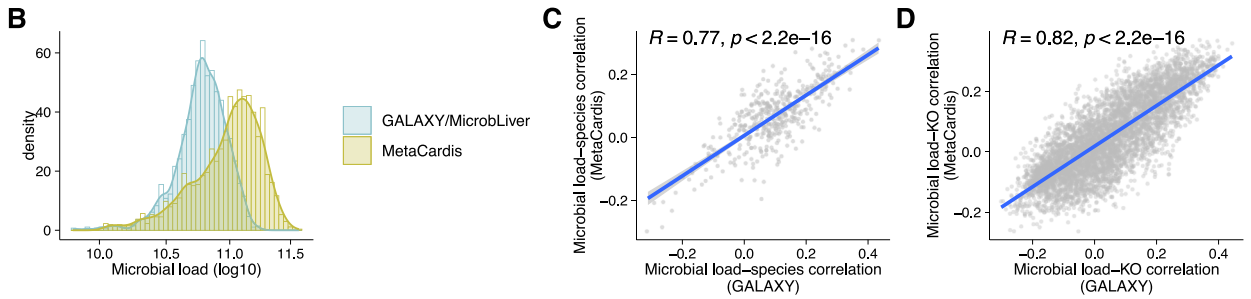

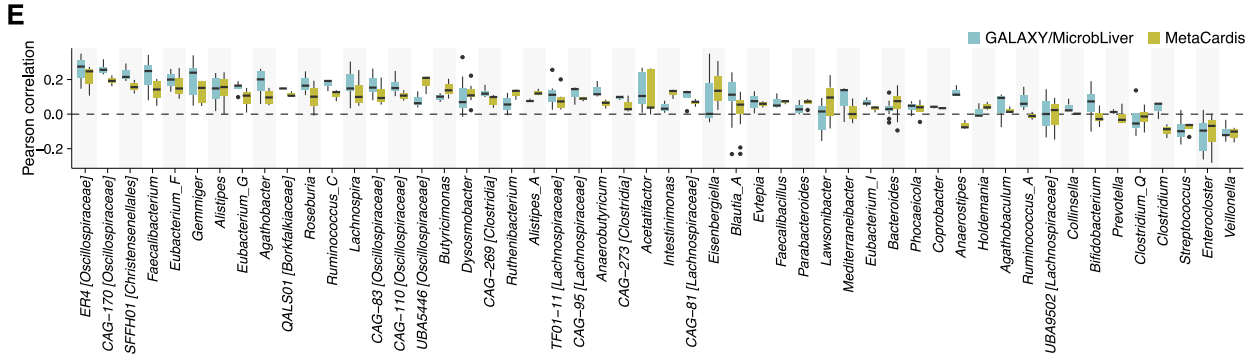

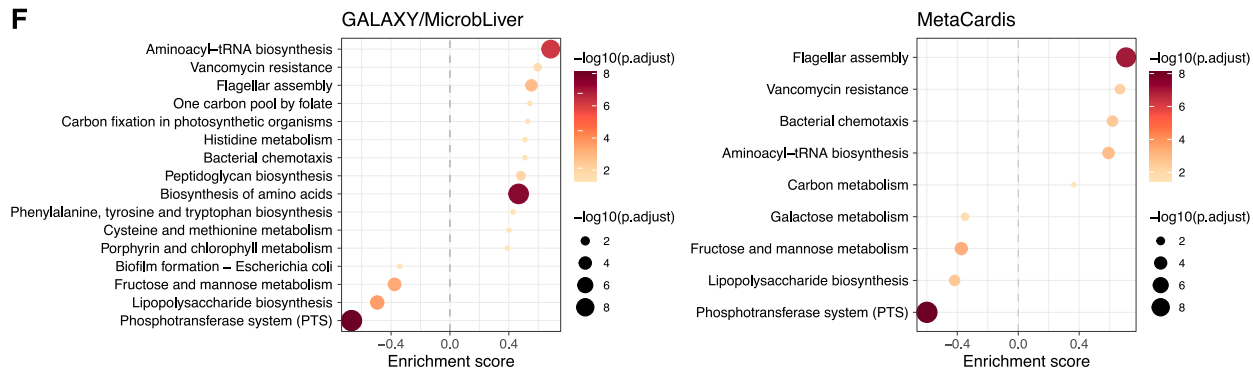

(legend on next page)

Figure S1. Overview of the analysis in this study and associations between microbial load and microbiome profiles in the GALAXY/MicrobLiver and MetaCardis study populations, related to Figure 1

(A) Flow chart of the analytical processes in this study.

(B) Comparison of microbial loads between the GALAXY/MicrobLiver (n = 1,894) and MetaCardis (n = 1,812) study populations.

(C and D) Comparison of microbial load-microbiome associations between the GALAXY/MicrobLiver and MetaCardis study populations. Each circle represents microbial species (C) and gene function based on KEGG orthology (D). Pearson correlation coefficient was employed to evaluate the correlations. For the species analysis, those with a mean relative abundance of >0.01% and prevalence of >10% in both studies were included. For the gene function analysis, KEGG orthologies with mean relative abundance of 0.0001% and prevalence of >10% in both studies were included.

(E) Species-microbial load correlations summarized at the genus level retrieved from the Genome Taxonomy Database (GTDB).

(F) Pathway enrichment analysis for genes associated with microbial load. Based on the Pearson correlation coefficients between gene functions and microbial load, over-representations of KEGG pathways in the positively and negatively associated genes were assessed using the gene set enrichment analysis (GSEA) function in the clusterProfiler package. Pathways showing statistical significance of FDR < 0.1 are shown in the plot.

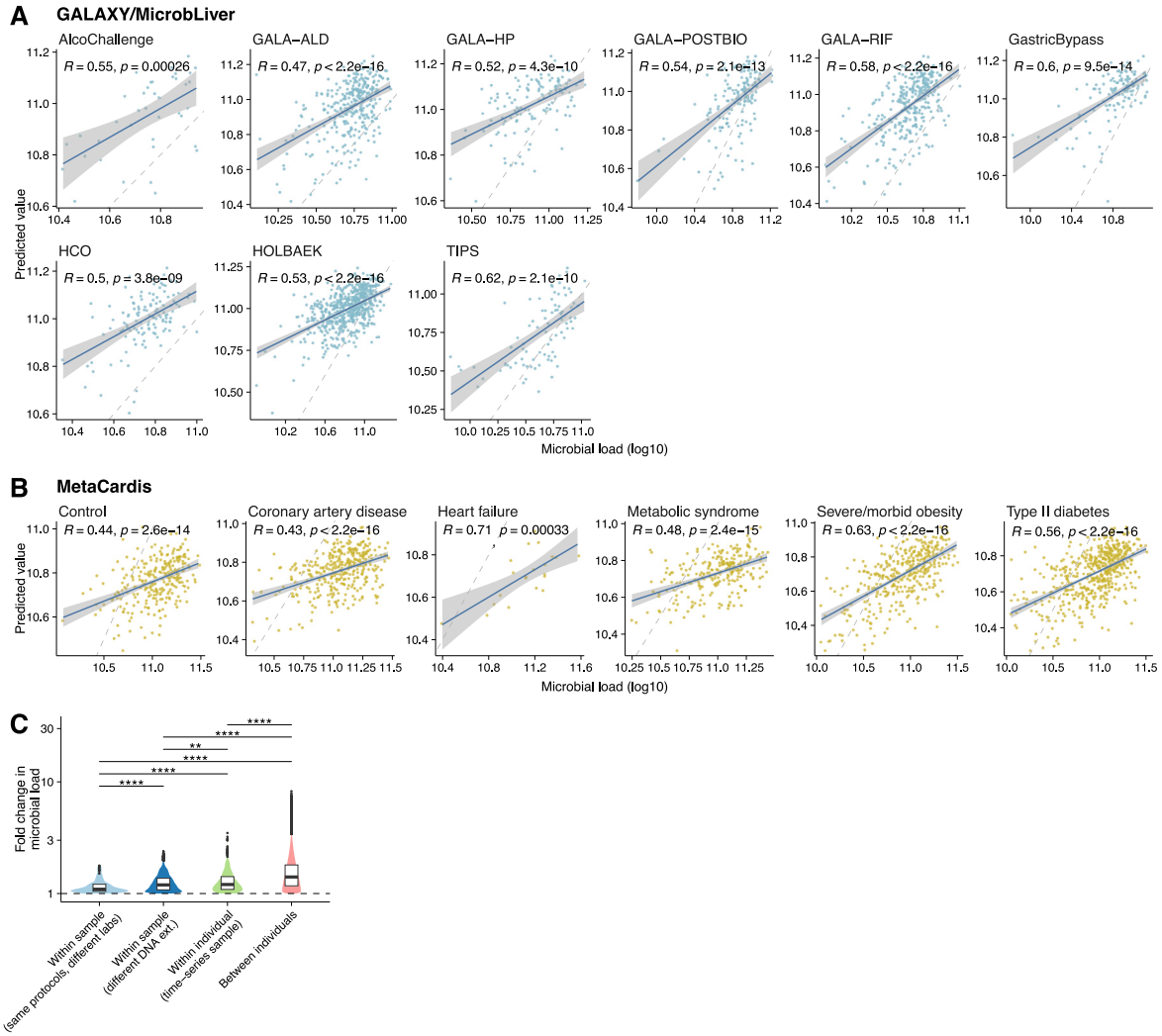

Figure S2. Evaluation of the robustness of the prediction models to biological and technical factors, related to Figure 2

(A and B) Scatterplots showing correlations between experimentally measured microbial loads and predicted values across sub-cohorts in the GALAXY/MicrobLiver study population (A) and various disease subgroups in the MetaCardis study population (B). XGBoost regression models trained on the species-level taxonomic profiles were applied to each other's datasets of the GALAXY/MicrobLiver and MetaCardis study populations. Numbers of individuals included in each sub-cohort and subgroup are as follows: AlcoChallenge, $n = 39$; GALA-ALD, $n = 333$; GALA-HP, $n = 127$; GALA-POSTBIO, $n = 161$; GALA-RIF, $n = 317$; GastricBypass, $n = 129$; HCO, $n = 125$; HOLBAEK, $n = 579$; TIPS, $n = 84$ (A), and control, $n = 275$; patients with coronary artery disease, $n = 361$; heart failure, $n = 21$; metabolic syndrome, $n = 246$; severe/morbid obesity, $n = 373$; and type II diabetes, $n = 536$ (B). The solid blue line shows regression lines, and the gray dashed lines represent 1:1 reference lines. The shadow of the regression line represents a 95% confidence interval. Pearson correlation coefficients are represented in the plots. Pearson correlations between experimentally measured and predicted microbial loads are shown with p values.

(C) Comparison of the effects of technical and biological factors on the predicted microbial load. The MetaCardis prediction model was applied to metagenomes sequenced in different laboratories with the same protocols (i.e., technical replicates), those obtained from the same samples with different DNA extraction methods, longitudinal samples from the same individuals, and those obtained from different individuals in previous studies. Absolute values of $\log_2$ fold change were calculated between each pair (i.e., within the same sample or individual) or between different individuals and compared between groups. ****$p < 0.0001$, ***$p < 0.001$, **$p < 0.01$ (Wilcoxon rank-sum test).

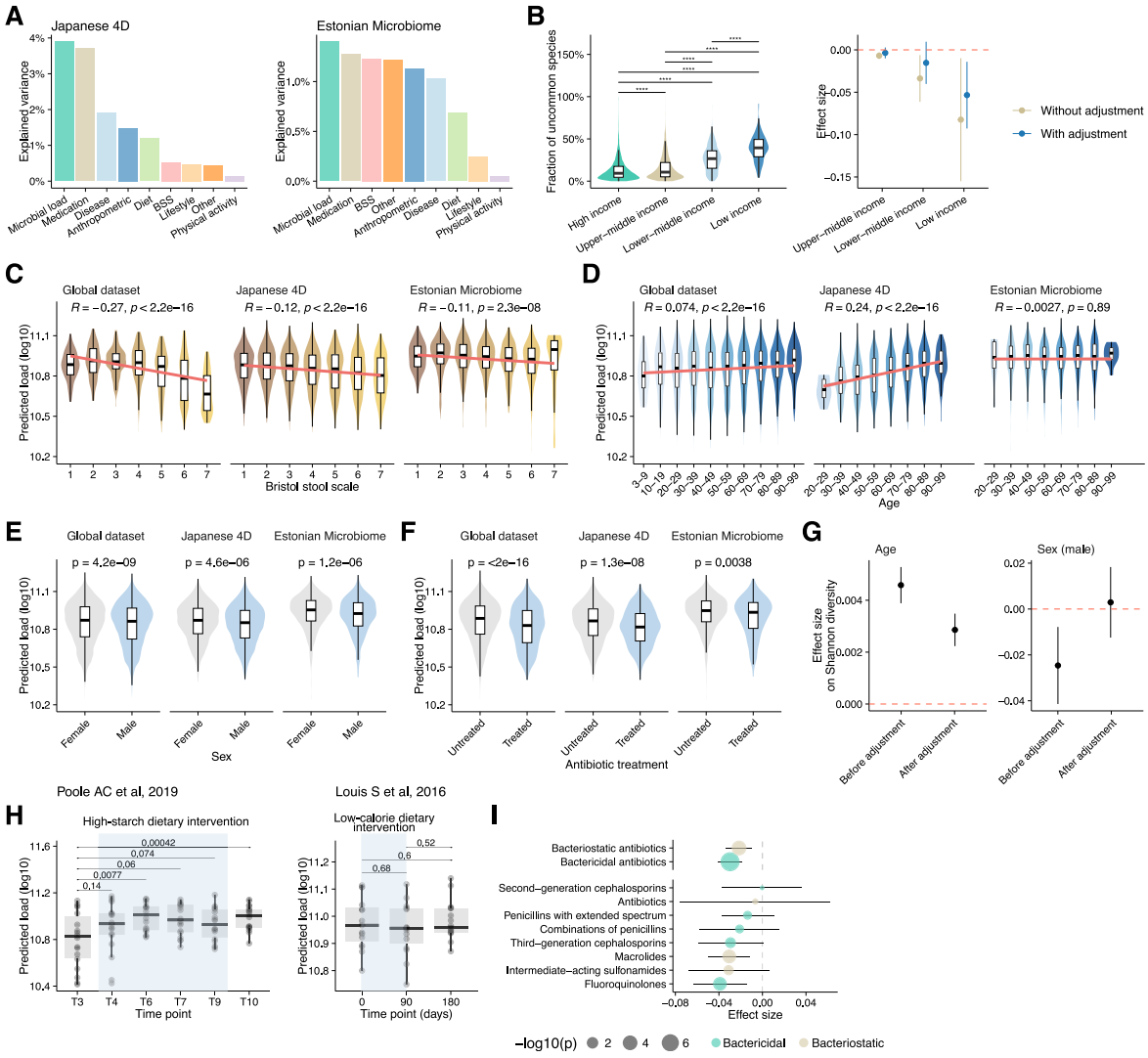

Figure S3. Associations between predicted microbial load and various host and environmental factors, related to Figure 3

(A) Associations between microbiome variation and various host and environmental factors, including predicted microbial load in the Japanese 4D (n = 4,198) and Estonian Microbiome cohorts (n = 2,509). The association between microbiome variation (the Bray-Curtis dissimilarity) and each metadata category was assessed based on distance-based redundancy analysis using the dbrda function in the vegan package.

(B) Total abundance of species not incorporated into the prediction model for each category of the country classified by economy (i.e., fraction of uncommon species in high-income countries) (left) and the effect of the category (relative to high-income countries) on the predicted microbial load when the fraction was incorporated into the model as a covariate (right). Error bars indicate 95% confidence intervals. ****p < 0.0001, ***p < 0.001 (Wilcoxon rank-sum test).

(C–F) Associations between the predicted microbial loads and the Bristol stool scale (C), host age (D), host sex (E), and antibiotic treatment (F) in the global dataset, Japanese 4D, and Estonian Microbiome cohorts. Pearson correlations (C and D) and Wilcoxon rank-sum test (E and F) were used to evaluate the associations.

(G) Effect sizes of host age and sex for Shannon diversity of the microbiome in the global and Japanese 4D datasets before and after the adjustment with the predicted microbial loads. The effect size was obtained using linear regression analysis, including Shannon diversity as the response variable and age and sex as the explanatory variable with and without the predicted microbial load as a covariate. Error bars represent the 95% confidence interval of the effect size.

(H) Changes in the predicted microbial load in two dietary intervention studies. In the study of Poole et al.,[54] samples were collected at six time points from 18 individuals. A high-starch dietary intervention was administered before time point T4 and finished after time point T9. In the study of Louis et al.,[138] samples were collected at three time points from 15 subjects, with a low-calorie dietary intervention conducted between time points 0 and 90. p values are indicated in the plot (Wilcoxon rank-sum test).

(I) Effects of different types of antibiotics on the predicted microbial load in the Japanese 4D and Estonian Microbiome cohorts. Each circle shows the effect size determined by a linear regression analysis, and the error bar represents 95% confidence intervals.

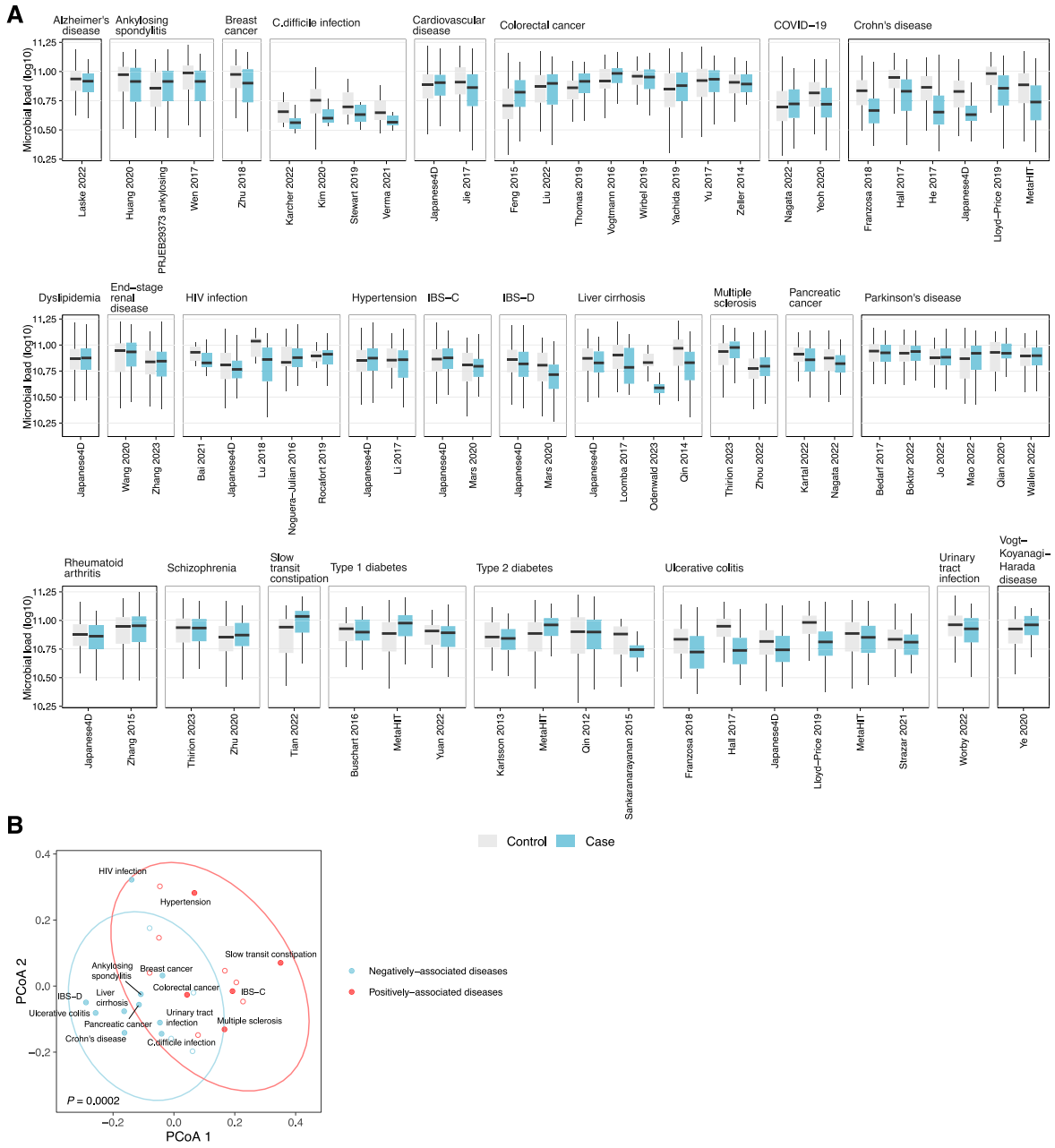

Figure S4. Associations between predicted microbial load and various diseases, related to Figure 4

(A) Boxplots comparing predicted microbial loads between disease cases and controls across the 26 diseases. 13,200 cases and 18,511 controls from 57 studies were included in the analysis (Table S4A).

(B) Principal coordinate analysis (PCoA) on microbial signature across the 26 diseases. Each circle represents each disease, and the blue and red colors show positively and negatively associated diseases with the predicted load, respectively. Microbial signatures of each disease were defined as the set of effect sizes of each species as determined using a linear regression analysis, with species abundances as the response variable and disease condition as the explanatory variable (see STAR Methods). The similarity of the microbial signatures between diseases was calculated using Spearman correlations, and they were transformed into distance. Principal coordinate analysis was performed on the distance matrix of the disease signature using the cmdscale function in the vegan package. The *p* value was calculated based on permutational analysis of variance using the adonis function in the vegan package.

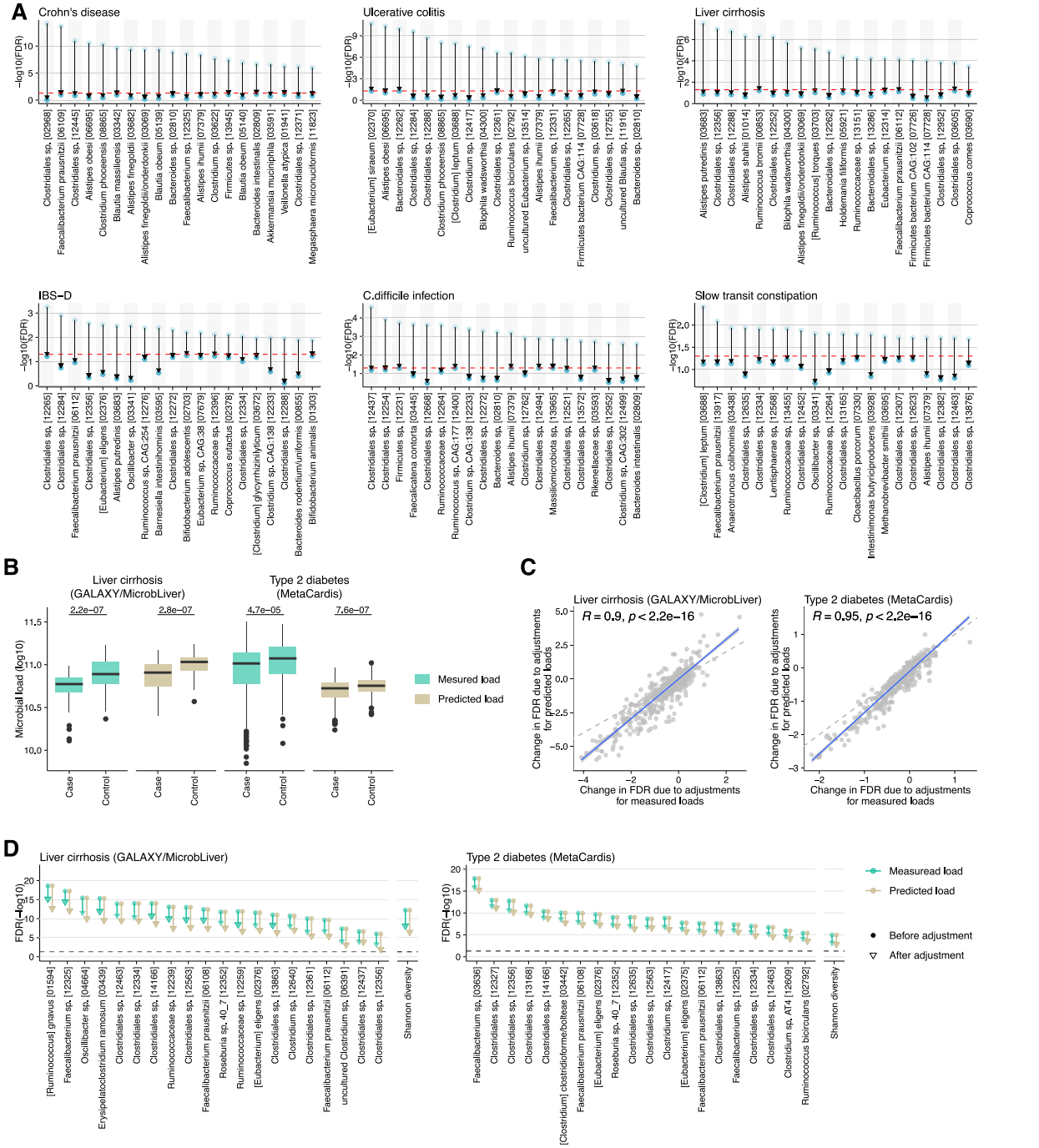

Figure S5. Adjusting for microbial load substantially changes the association between microbiome-disease associations, related to Figure 5

(A) Species that lost statistically significant associations with diseases after the adjustment for microbial loads (FDR > 0.05). The associations between a species and a disease were evaluated using linear regression analysis with and without the adjustment. The red horizontal lines show an FDR of 0.05. Arrows represent the changes in the FDR before to after the adjustment for microbial load. Results for the six diseases, for which the adjustment had the strongest impact, are included in the plot. The top 20 species with the lowest FDR before the adjustment are shown. Results for breast cancer are not shown since only four significant species were detected.

(B) Comparison of experimentally measured and predicted microbial loads between patients and controls in the GALAXY/MicrobLiver and MetaCardis study populations. Patients with liver cirrhosis (n = 64) and healthy controls (n = 127) were selected from the GALAXY/MicrobLiver study population, and patients with type 2 diabetes (n = 539) and healthy controls (n = 275) were selected from the MetaCardis study population. Predicted microbial loads were obtained by applying the MetaCardis and GALAXY/MicrobLiver models to each other's datasets. Numbers in the plot represent the p values between cases and controls (Wilcoxon rank-sum test).

(legend continued on next page)

(C) Comparison of changes in FDR values (log_{10} transformed) for each microbial species due to adjustment for measured and predicted microbial loads. Pearson correlation was employed to evaluate associations between them.
(D) Changes in FDR values after the adjustment for each microbial species and Shannon diversity. Results for the top 20 microbial species with the largest reduction in FDR and Shannon diversity are shown in the plot.

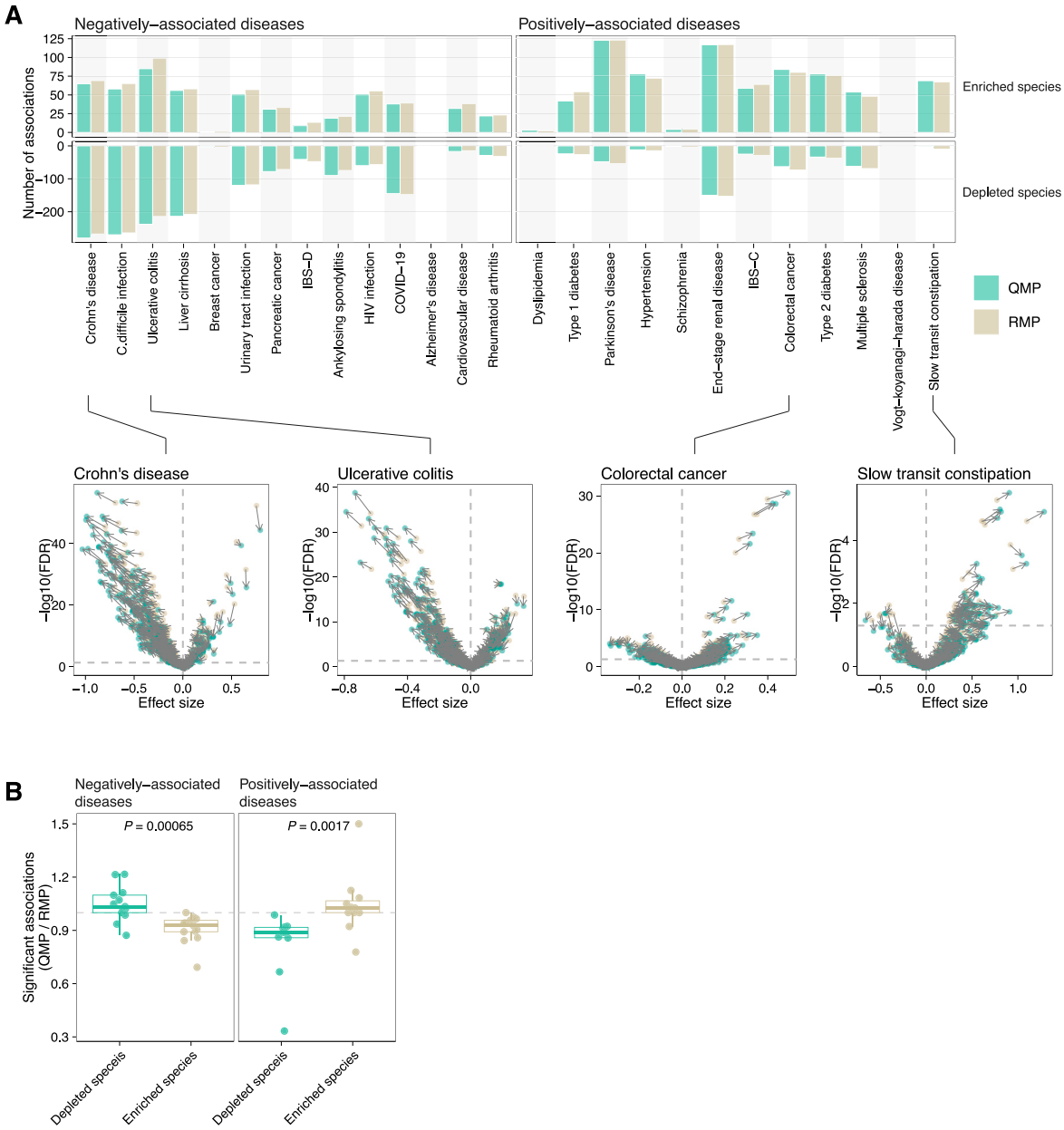

Figure S6. Predicted microbial load partially reduces biases derived from the relative nature of the microbiome data, related to Figure 5

We compared the results of case-control analyses of each disease between the relative microbiome profile (RMP) (i.e., a profile where species abundances were represented by relative abundance) and the quantitative microbiome profile (QMP) (i.e., a profile where species abundances were represented by absolute abundances by taking into account the predicted microbial load) (see STAR Methods).

(A) Bar plot showing the number of significantly enriched and depleted species (FDR < 0.05). The volcano plot below shows the effect sizes and FDRs of each species for Crohn's disease, ulcerative colitis, colorectal cancer, and slow transit constipation as examples. Arrows represent the shift of the results from the RMP to QMP.

(B) Boxplot showing the ratio of the number of significant species (FDR < 0.05) between the RMP and QMP data. Wilcoxon rank-sum test was used to compare the ratio between depleted and enriched species. In negatively associated diseases such as Crohn's disease and ulcerative colitis, the majority of depleted species in the patients increased their effect size and statistical significance in the QMP compared with the RMP, while enriched species decreased the statistical significance. It was the opposite in the positively associated diseases such as colorectal cancer and slow transit constipation. These results indicate that RMP-based analyses underestimate or overestimate disease-associated microbial species due to differences in microbial load between cases and controls, while QMP-based analyses reduce these biases.